Hamburger Beiträge
zur Angewandten Mathematik

Interior Point Methods in Function Space for State Constraints - Inexact Newton and Adaptivity

Anton Schiela and Andreas Günther

Nr. 2009-01
January 2009

Interior Point Methods in Function Space for State Constraints - Inexact Newton and Adaptivity

Anton Schiela* & Andreas Günther†

January 16, 2009

Abstract

We consider an interior point method in function space for PDE constrained optimal control problems with state constraints. Our emphasis is on the construction and analysis of an algorithm that integrates a Newton path-following method with adaptive grid refinement. This is done in the framework of inexact Newton methods in function space, where the discretization error of each Newton step is controlled by adaptive grid refinement in the innermost loop. This allows to perform most of the required Newton steps on coarse grids, such that the overall computational time is dominated by the last few steps. For this purpose we propose an a-posteriori error estimator for a problem suited norm.

AMS MSC 2000: 90C51, 49M05

Keywords: interior point methods, function space, adaptivity, state constraints

1 Introduction

This work deals with the efficient solution of optimal control problems with partial differential equations, subject to pointwise state constraints. These problems form a class of highly nonlinear problems in function space. The main algorithmic approaches thus introduce certain regularizations to solve problems efficiently. However, the aim is still to obtain the solution of the original problem up to a certain accuracy. So the regularizations have to be reversed step by step, and thus during the course of the algorithm the subproblems that have to be solved can be expected to become harder and harder. This leads to the use of path-following algorithms and their analysis in function space.

While a sound convergence theory in function space yields confidence on the efficiency of algorithms and ideas for the details of their construction, of course, any computer algorithm for problems in function space must *discretize* the problems at some point. For the sake of efficiency the discretization should be as coarse as the accuracy requirements allow. However, it is hard to judge a-priori, which discretization is appropriate. This may only become clear in the course of the algorithm. These effects are particularly important in the context of state constrained optimal control, because near the constraints strongly local effects are to be expected, but their location can hardly be predicted a-priori.

*Konrad-Zuse-Zentrum für Informationstechnik Berlin, Takustraße 7, 14195 Berlin, Germany. Supported by the DFG Research Center Matheon "Mathematics for key technologies".

†Bereich Optimierung und Approximation, Universität Hamburg, Bundesstraße 55, 20146 Hamburg, Germany.

So discretizations should be adjusted to the problem during the run-time of the algorithm. Even more, in path-following methods where the subproblems become harder and harder, it is important to have good starting values for the subproblems in *function space*. Only this guarantees robustness of an algorithm with respect to grid changes, and ensures that the discrete algorithm inherits the properties of its continuous counterpart. As a desirable side-effect, successive grid refinement during an algorithm improves efficiency drastically, because large scale problems only appear towards the end. Then the overall computational time is dominated by the last (few) step(s).

In this work we describe an algorithmic approach to implement these ideas in the framework of an interior point method in function space. The structure of our algorithm is sketched in Figure 1. It consists of three nested loops: a path-following scheme, a Newton corrector, and the approximate solution of an operator equation. The crucial point is that the two outer loops are performed inexactly in *function space*, and discretization takes place in the innermost loop. This idea has already been applied to several classes of problems [27, 18, 41, 42, 35, 17]. It contrasts so called "nested iteration schemes", where discretizations are refined in an outer loop, and discrete (and often mesh-independent) algorithms are used to solve the discretized problems. While our main emphasis are interior point methods, parts of this paper are written in a more general way, so that the results can also be applied to other classes of algorithms. In particular in Section 3 some, but not all results apply to semi-smooth Newton methods as well.

Of particular interest is the interplay between nonlinearity and discretization. For state constrained optimal control problems it turns out that the use of problem suited norms in the framework of inexact Newton methods is important. Surprisingly (at the first sight), there are good discretization error estimates available just for these "natural" norms. The deeper reason is, of course, that the nonlinearity of the original problem has effects on *all* components of the solution algorithm – from the analytic properties of the homotopy path via convergence radii for Newton's method to the construction of a-posteriori error estimates.

Let us shortly outline the related literature. For elliptic, pointwisely state constrained optimal control problems analysis and regularity investigations were carried out in [10, 11, 2]. The papers [12, 13] provide finite element error estimates for semilinear elliptic equations with finitely many state constraints. Further extensions as dealing with additional control constraints, discretizing with piecewise constant controls as well as error estimates in two and three space dimensions are covered in [14, 15, 16] and [30].

Now let us consider adaptive concepts for state constrained elliptic optimal control. Residual-type a-posteriori error estimators are investigated in [28]. Apart from that the motivation to design optimal meshes with respect to a certain goal is based on the DWR method established in [7, 8]. This technique of goal-oriented adaptivity is extended to state constraints within [21, 22]. In [9] the furthermore elliptic semilinear equations are considered.

Path-following in function space is a rather popular approach to the solution of state constrained problems, and the authors are aware of three main lines of research. Well known are the so called Moreau-Yoshida regularization methods [24], Lavrentiev regularization [31, 32] and interior point methods [36, 37, 38]. For all three methods, an analysis of the homotopy path is available, and path-following algorithms have been proposed, based on Newton's method, sometimes in the semi-smooth variant. A proof of convergence for an interior point path-following method has been found in [39].

Discretization error estimates for interior point methods for state constraints were proved in [26]. Recently in [45] a way to merge interior point methods and classical goal oriented error estimation was proposed. The aim was here to balance the errors in the objective

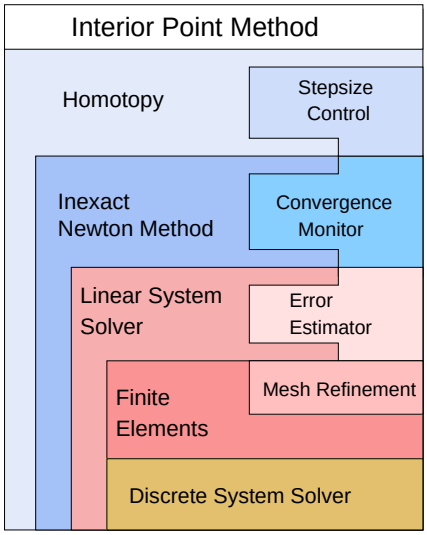

Figure 1: Structure diagram of a practical path-following algorithm.

functional that arise from discretization and regularization. In contrast to this, our grid refinement strategy is driven by the requirement to stay in the region of Newton contraction in function space. Both approaches complement each other, and may possibly used in combination.

Our paper is structured as follows: in Section 2 we briefly sketch our analytic framework and the main ideas and results about interior point path-following methods for state constraints, achieved so far. We demonstrate that elliptic partial differential equations fit into this framework. We proceed in Section 3 with a discussion of an inexact Newton corrector for our scheme. Special emphasis is set on the comparison of exact and perturbed (discretized) Newton steps. We discuss conditions for which the inexact iteration asymptotically inherits the behavior of the exact method. Further we propose a computable convergence criterion for Newton's method that is used to compute an update of the homotopy parameter. This update strategy is discussed in Section 4. It takes into account the above mentioned convergence criterion and tangential information of the homotopy path. Finally in Section 5 we prove a general result for the representation of the error in function space measured in a natural norm. Applying this result to a concrete optimal control problem from Section 2 and using standard techniques from a-posteriori error estimation leads to the definition of an a-posteriori error estimator for the error with respect to this natural norm. Finally, we investigate the performance of our algorithm by some numerical examples.

Acknowledgment. The authors want to thank Dr. Martin Weiser for constructive discussions and close cooperation concerning the numerical implementations with finite elements. Further, they want to thank Prof. Dr. Michael Hinze for helpful discussions and support.

The work of the first author was supported by the DFG Research Center MATHEON "Mathematics for key technologies". The second author acknowledges support of the DFG Priority Program 1253 through grants DFG06-381 and DFG06-382.

2 Interior Point Methods in Function Space

In [37, 38, 39] interior point methods in function space were analyzed and an algorithm in function space was given. We recapitulate the main results from these works. The theoretical results in this paper are motivated by interior point methods, and can be applied inside their theoretical framework.

2.1 Formal Framework

Let Ω be an open and bounded domain in $\mathbb{R}^d$, $d \in \{1, 2, 3\}$ and $\overline{\Omega}$ its closure. Let Y denote the space of states and U the space of controls. Define $Z := Y \times U$ with $z := (y, u)$ and consider the following convex minimization problem, the details of which are fixed in the remaining section.

$$\begin{aligned} \min_{z \in Z} J(z) \quad & \text{s.t. } Ay - Bu = 0 \\ & \underline{y} \leq y. \end{aligned} \tag{1}$$

We set $Y = C(\overline{\Omega})$ (or a closed subspace thereof), and $U = L_2(Q)$ for a measurable set Q equipped with an appropriate measure. Our setting will include, for example, optimal control problems subject to linear elliptic partial differential equations with distributed control ($Q = \Omega$), boundary control ($Q = \partial\Omega$, for $d \leq 2$) and finite dimensional control ($Q = \{1, \ldots, n\}$, equipped with the counting measure).

We will now specify our abstract theoretical framework, which holds throughout this work and collect a couple of basic results about this class of problems.

A Convex Functional. For simplicity, let J be a quadratic tracking type functional with quadratic control cost. Let $\alpha > 0$ and $y_d \in L^2(\Omega)$ and define

$$J(z) = \frac{1}{2} \|y - y_d\|_{L_2}^2 + \frac{\alpha}{2} \|u\|_{L_2}^2 .$$

Obviously, this functional is strictly convex and differentiable in Z, with derivative $J'(z) = (y - y_d, \alpha u)$.

Inequality Constraints. We assume that $\underline{y} \in C^{1,1}(\overline{\Omega})$, which means that its spacial derivatives are Lipschitz continuous. The inequality constraints in (1) are interpreted to hold pointwisely almost everywhere and they define the closed subset of $Y \times U$ of all pairs (y, u) that satisfy $\underline{y} \leq y$ a.e. in Ω. We assume that there is a *strictly feasible point* $\breve{z} = (\breve{y}, \breve{u})$ that satisfies $A\breve{y} - B\breve{u} = 0$ and

$$0 < d_{\min} := \operatorname{ess\,inf}_{t \in \overline{\Omega}} \{\breve{y}(t) - \underline{y}(t)\}. \tag{2}$$

We call such a condition a (uniform pointwise) *Slater condition* and $\breve{z}$ a *Slater point*. This condition together with the topology of Y defined by $\|\cdot\|_\infty$ is used in the analysis of dual variables and subdifferentials and in the derivation of first order optimality conditions (cf. [37]).

Equality Constraints. The equality constraint $Ay - Bu = 0$ is introduced to model a partial differential equation (cf. Section 2.2 for an example).

Let P be a reflexive Banach space and $B : U \to P^*$ be continuous. We assume that $A : Y \supset \operatorname{dom} A \to P^*$ is a linear operator, which is *densely defined, closed* and maps $\operatorname{dom} A$ to P^* *bijectively*.

Our assumptions on A are essentially equivalent to the existence of a continuous inverse A^{-1}. In the context of optimal control P is often a Sobolev space and the operator B is usually defined as the adjoint of an embedding or a trace operator (cf. e.g. the discussion in [26] or [38]).

We consider A as a model of a differential operator (for an example, cf. Section 2.2 below), which may be unbounded. Closed, densely defined operators between Banach spaces are a classical concept of functional analysis with numerous applications. They are more flexible than continuous operators but retain much of their structure. In particular, there is an open-mapping theorem, a closed range theorem, and adjoint operators are well defined. In this work and in [37, 38] only these basic properties of A are needed for a successful analysis. A classical introduction to unbounded operators is [20], but most elementary facts can also be found in standard textbooks on functional analysis ([44, 46]). Our main motivation for their use here is that the nonlinearity of state constraints requires to use spaces of *continuous functions* (therefore our choice $Y = C(\overline{\Omega})$), but differential operators can only be defined on spaces of smooth functions. Unbounded operators allow us to combine both apparently conflicting requirements elegantly, and in a very flexible way.

On Banach spaces, closed, bijective operators have a continuous inverse (by the open mapping theorem), and operators with a continuous inverse are automatically closed (cf. e.g. [39, Lem. 2.1]). Hence, our assumption of closedness of A holds, if the solution operator $A^{-1} : P^* \to \operatorname{dom} A \subset C(\overline{\Omega})$ is continuous.

We exploit density of $\operatorname{dom} A$ in Y to define an adjoint operator A^* by the following standard construction. Here and in the following we denote by $\langle \cdot, \cdot \rangle$ the dual pairing. For every $p \in P$ the mapping $y \to \langle p, Ay \rangle$ is a linear functional on $\operatorname{dom} A$. We define $\operatorname{dom} A^*$ as the subspace of all $p \in P$ for which $y \to \langle p, Ay \rangle$ is *continuous* on $\operatorname{dom} A$. Every $p \in \operatorname{dom} A^*$ can thus be extended uniquely to a continuous functional on Y by density of $\operatorname{dom} A$ in Y. Hence, for each $p \in \operatorname{dom} A^*$ there is a unique linear functional $A^* p \in Y^*$ for which

$$\langle p, Ay \rangle = \langle A^* p, y \rangle \qquad \forall\, y \in \operatorname{dom} A. \tag{3}$$

This yields the definition of $A^* : P \supset \operatorname{dom} A^* \to Y^*$. Because P is reflexive, $\operatorname{dom} A^*$ is dense in P. This is due to [20, Thm. II.2.14].

Existence of Optimal Solutions. Existence of optimal solutions follows by standard arguments: because A^{-1} is continuous we can eliminate $y = y(u) = A^{-1}Bu$, and consider the problem $\min J(y(u), u)$ subject to $y(u) \geq \underline{y}$. This is an optimal control problem on a closed subset of the reflexive space U with a convex, continuous and coercive functional. Thus we can apply a well known theorem (cf. e.g. [19, Prop. II.1.2]) on existence of a minimizer u_{opt}, and thus of a minimizer $z_{opt} = (y(u_{opt}), u_{opt})$ of (1). Since J is even strictly convex, z_{opt} is unique.

2.2 An Elliptic Differential Operator

In order to have a concrete class of problems at hand we consider as an example optimal control problems subject to an elliptic partial differential equation on a domain $\Omega \subset \mathbb{R}^d$. For this case consider A of the form

$$\langle Ay, w \rangle = \int_\Omega \langle \kappa \nabla y, \nabla w \rangle + ayw \, dt, \tag{4}$$

where we impose the usual assumptions of ellipticity and boundedness of the tensor $\kappa = \kappa(t)$, non-negativity and boundedness of a, assuming that a is non-zero on a set of positive measure. The most natural functional analytic framework for A is certainly $A : H^1(\Omega) \to (H^1(\Omega))^*$. Then $\langle Ay, w\rangle$ is defined by (4) for all $v, w \in H^1(\Omega)$. By the Lax-Milgram theorem A is an isomorphism.

However, since in most cases of interest $H^1(\Omega) \not\hookrightarrow C(\overline{\Omega})$, which is crucial for state constraints, we have to consider a different set of spaces. We define for $1 < s < \infty$ and its conjugate exponent $s' := s/(s-1)$

$$A : W^{1,s}(\Omega) \to (W^{1,s'}(\Omega))^*, \tag{5}$$

where $\langle Ay, w\rangle$ is defined by (4) for $y \in W^{1,s}(\Omega)$ and $w \in W^{1,s'}(\Omega)$. Under suitable (mild) regularity assumptions on the coefficients and the boundary of the domain regularity results imply that A is still an isomorphism for some $s > d$ (cf. e.g. [4, Thm. 9.2]). By the Sobolev embedding theorems there is the continuous (and dense) embedding $W^{1,s}(\Omega) \hookrightarrow C(\overline{\Omega})$, and thus

$$A : C(\overline{\Omega}) \supset W^{1,s}(\Omega) \to (W^{1,s'}(\Omega))^* \tag{6}$$

is well defined and continuously invertible, hence closed and bijective (cf. [39, Lem. 2.1]) and fits thus into our framework with $P = W^{1,s'}(\Omega)$. Observe that (5) and (6) define the same algebraic mapping, but the topology of the domain is chosen differently. Namely, (6) is suited to the needs of optimal control theory.

Using the fact that the space of Radon measures $M(\overline{\Omega})$ is the representation of $C(\overline{\Omega})^*$, the adjoint operator of A is defined just as described in the preceeding section via

$$A^* : W^{1,s'}(\Omega) \supset \operatorname{dom} A^* \to M(\overline{\Omega}),$$

and $\langle y, A^* w\rangle = \langle Ay, w\rangle$ for all $y \in W^{1,s}(\Omega)$ and $w \in \operatorname{dom} A^*$. Further, let us note that for any $s > d$, there is also the continuous Sobolev embedding $W^{1,s}(\Omega) \to C^\beta(\Omega)$ with some $\beta > 0$, depending on s. This means that in this example all states can be considered Hölder continuous.

For the operator $B : U \to P^*$, there are several choices possible. For example, distributed control is modelled by $U = L_2(\Omega)$ and $\langle Bu, w\rangle = \int_\Omega uw\, dt$, boundary control by $U = L_2(\partial\Omega)$ and $\langle Bu, w\rangle \int_{\partial\Omega} u\gamma(w)\, dS$. Here $\gamma : W^{1,s'}(\Omega) \to L_2(\partial\Omega)$ is the boundary trace operator, which is well defined for spacial dimension $d \le 2$.

2.3 Barrier Regularization

The simple idea of interior point or barrier methods is to replace the state constraints by a barrier functional $b(\cdot;\mu)$, that tends to ∞, if the state approaches the lower bound $\underline{y}$. For its construction we consider logarithmic or rational barrier functions.

Definition 2.1. For given $q \ge 1$, $\mu > 0$, $\underline{y} \in \mathbb{R}$ the functions $l(y;\mu) :]\underline{y};\infty[\to \overline{\mathbb{R}}$ defined by

$$l(y;\mu) := \begin{cases} -\mu \ln(y - \underline{y}) & : \quad q = 1 \\ \dfrac{\mu^q}{(q-1)(y-\underline{y})^{q-1}} & : \quad q > 1 \end{cases}$$

are called *barrier functions of order q*. We extend their domain of definition to $\mathbb{R}$ by setting $l(y;\mu) = \infty$ for $y \le \underline{y}$.

Using these barrier *functions* $l(y;\mu)$ we construct barrier *functionals* $b(y;\mu)$ to implement constraints of the form $y \geq \underline{y}$ on a measurable set $Q \subset \overline{\Omega}$ (equipped with a finite and regular positive measure) by computing the integral over l:

$$\begin{aligned} b(\cdot;\mu) : C(Q) &\to \overline{\mathbb{R}} \\ y &\mapsto \int_Q l(y(t);\mu)\, dt. \end{aligned}$$

Observe that for a given function $\underline{y}$, the integrand depends also on $\underline{y}(t)$, so more accurately, $l(y(t);\mu) = l(y(t);\underline{y}(t);\mu)$. For reasons of notational brevity we suppress this dependence. Of course, $b(\cdot;\mu)$ can be defined as a functional on Z, which is independent of u.

It has been shown in [37] that the barrier problems

$$\min_{z\in Z} J(z) + b(y;\mu) \;\text{ s.t. }\; Ay - Bu = 0 \tag{7}$$

are well defined for each $\mu > 0$ and admit a unique minimizer $z(\mu) = (y(\mu), u(\mu))$ in the formal framework of this paper. Further, the path of minimizers, the *central path*, converges to the solution of the original problem $z_{opt} = (y_{opt}, u_{opt})$ with a rate of convergence

$$\|z(\mu) - z_{opt}\| = O(\sqrt{\mu}), \tag{8}$$

and is locally Lipschitz continuous with Lipschitz constant $L(\mu) \leq O(\mu^{-1/2})$.

Minimizers admit first order optimality conditions, which in case of *strict feasibility* of the state read:

$$\begin{aligned} y - y_d + b'(y;\mu) + A^*p &= 0 \\ \alpha u - B^*p &= 0 \\ Ay - Bu &= 0. \end{aligned} \tag{9}$$

Here b' is defined via

$$\langle b'(y;\mu), \delta y\rangle = \int_Q l'(y;\mu)\delta y\, dt.$$

Strict feasibility can be guaranteed a-priori, if $y \in C^\beta(\overline{\Omega})$ for some $\beta > 0$, and the order q of the barrier function is chosen sufficiently large (cf. [37]). We will assume this setting in our remaining considerations.

2.4 Interior Point Path-following

Elimination of u from (9) yields the system of equations

$$\begin{aligned} y - y_d + b'(y;\mu) + A^*p &= 0 \\ -Ay + \alpha^{-1}BB^*p &= 0 \end{aligned} \tag{10}$$

which will be the basis for our path-following algorithm (cf. Algorithm 2.3). We combine the variables $x := (y, p)$, and denote the left hand side of (10) by $F(\cdot;\mu) : Y\times P \supset D \to Y^*\times P^*$. Defining $X := Y \times P$ and $R := Y^* \times P^*$, we will use the general notation

$$F(\cdot;\mu) : X \supset D \to R.$$

For each $\mu > 0$, the unique zero of (10) will be denoted by $x(\mu) = (y(\mu), p(\mu))$.

In each call of "InexactNewtonCorrector($x_j;\mu_j$)" in Algorithm 2.3 we solve the system (10) of equations approximately by an inexact variant of Newton's method, which we will consider in detail in Section 3. This is performed for an adaptively chosen sequence $\mu_j \to 0$ (cf. Section 4).

The formal linearization of $F(x;\mu)$, defined by (10) reads

$$F'(x;\mu) := \begin{pmatrix} I + b''(y;\mu) & A^* \\ -A & \alpha^{-1}BB^* \end{pmatrix}. \tag{11}$$

For a given point $x_- \in D$ and $\mu > 0$, the result x of an exact Newton step in function space is given by

$$x := x_- - F'(x_-;\mu)^{-1}F(x_-;\mu).$$

It has been shown in [39] that a simple Newton path-following algorithm in function space (similar to Algorithm 2.3), controlled appropriately, yields a sequence of iterates x_j that converges, such that $(y_j, \alpha^{-1}B^*p_j)$ converges to z_{opt}.

It is an important insight from [39] that a certain "natural" norm plays an important role, namely the norm induced by the diagonal of (11):

$$\|\delta x\|_{x;\mu} := \left\| \sqrt{1 + l''(y;\mu)}\delta y \right\|_{L_2} + \left\| \alpha^{-1/2}B^*\delta p \right\|_U. \tag{12}$$

Since $l''(y;\mu) \to \infty$ for $y \to \underline{y}$ the scaling inside this norm is large if the nonlinearity is high.

Of course, since y has to satisfy *pointwise bounds*, the norm $\|\cdot\|_\infty$ also plays a role. We define

$$|||\delta x|||_{x;\mu} := \|\delta x\|_{x;\mu} + \|\delta y\|_\infty. \tag{13}$$

The convergence of Newton's method during a path-following step can then be described as follows: if the initial value x (the predictor) is sufficiently close to $x(\mu)$ with respect to the $|||\cdot|||_{x;\mu}$-norm, then for the Newton iterates $|||x - x(\mu)|||_{x;\mu}$ remains small and the speed of convergence is governed by the weaker norm $\|\cdot\|_{x;\mu}$. The restriction with respect to $|||x - x(\mu)|||_{x;\mu}$ is essentially the requirement that the distance of the iterates to the bounds $y - \underline{y}$ is of similar size as $y(\mu) - \underline{y}$. In practice, $\|\cdot\|_{x;\mu}$ is used to control the algorithm, while a *pointwise damping step* enforces the requirement of strict feasibility. A more detailed discussion of these issues can be found in [39].

For later use we recall the following solvability theorem for the Jacobian matrix $F'(x;\mu)$. Observe that the inverse Jacobian has a strong *smoothing property.*

Theorem 2.2. *Let $\mu > 0$ and $x = (y,p) \in X$ be given. Assume that y is strictly feasible. For $r_a \in Y^*$ the system*

$$\begin{pmatrix} I + b''(y;\mu) & A^* \\ -A & \alpha^{-1}BB^* \end{pmatrix} \begin{pmatrix} \delta y \\ \delta p \end{pmatrix} = \begin{pmatrix} r_a \\ 0 \end{pmatrix} \tag{14}$$

admits a unique solution $(\delta y, \delta p) \in X$, with $\delta y \in \operatorname{dom} A$ and $\delta p \in \operatorname{dom} A^*$. The following estimate holds:

$$|||(\delta y, \delta p)|||_{x;\mu} \le C \sup_{v \in Y} \frac{\langle r_a, v\rangle}{|||(v,0)|||_{x;\mu}}. \tag{15}$$

Here C is independent of x and μ.

Proof. Cf. [39, Thm. 4.2]. □

Algorithm 2.3 (Path-following in Function Space)**.**
input: μ_0, x_0 *(Initial Guess)*
$j = 0$
do *(Homotopy Step)*
  $(\widetilde{x}$,success$) \leftarrow$ InexactNewtonCorrector$(x_j;\mu_j)$
  if success
    choose new μ_{j+1} (*cf. Section 4.3)*
    $x_{j+1} \leftarrow \widetilde{x}$
    $j \leftarrow j+1$
  else
    if $(j > 0)$ choose μ_j more conservatively
    else terminate: "bad initial guess"
while TotalError > DesiredTotalError

Figure 2: Sketch of a practical path-following algorithm.

3 An Inexact Newton Corrector in Function Space

Let us consider in detail an algorithm for the approximate solution of the homotopy subproblems in function space, i.e., the subroutine "InexactNewtonCorrector$(x_j; \mu_j)$" in Algorithm 2.3. The concept of inexact Newton in function space has been developed in a sequence of works [27, 18, 41, 42, 35] and is also considered in the monograph [17]. In this section, we will first study several aspects of this algorithm in a general framework, including, to some degree, semi-smooth problems. Then we will consider in detail a variant, particularly constructed for our interior point path-following method. Here and in the rest of the paper, we use the notation $[q]$ for a computable estimate of an analytic quantity q.

Consider Algorithm 3.2. Each step of the outer loop consists of an *inexact* Newton step in *function space*. The inexactness is unavoidable, since only discrete approximations (for example by finite elements) can be computed. However, with a-posteriori error estimation and adaptive grid refinement, these errors can be *controlled*. This is done in the inner loop of Algorithm 3.2. Note that the set of marked triangles is initialized as the empty set at the beginning of Algorithm 2.3. Then Algorithm 3.2 terminates with a set of marked triangles. These are refined at the beginning of the next corrector step.

Remark 3.1. In the work [24] the term *inexact path-following algorithm* is used to express the fact that the Newton *corrector* for the discrete problem is terminated after a certain accuracy requirement has been reached. Because Newton's method is an iterative method, this feature is usually understood without mentioning. This notion should not be confused with *inexact Newton methods in function space* as considered here, where each *step* of the Newton corrector is computed to a certain accuracy in function space.

3.1 An Inexact Newton Step

Let a nonlinear equation $F(x) : X \supset D \to R$ with zero $x_* : F(x_*) = 0$ be given. For an appropriate starting value $x_- \in D$, it is the aim of a Newton step $x_- \to x$ to achieve an error reduction

$$\|x - x_*\| \le \beta \|x_- - x_*\| \quad \text{for some } \beta < 1. \tag{16}$$

In our setting x_* lies in function space, but the iterates are members of some finite element space. If (16) can be achieved inductively, then iterative application of Newton steps yields

Algorithm 3.2 (Inexact Newton Corrector)**.**
input: μ, x_- *(Initial Guess)*
do *(Newton Step)*
  do *(Adaptive Refinement)*
    RefineMarkedTriangles
    $x \leftarrow x_- - F_h'(x_-;\mu)^{-1} F_h(x_-;\mu)$
    $[\|e\|_{x_-;\mu}] \leftarrow$ ErrorEstimator:Discretization(x) *(cf.* (58)*)*
    MarkTriangles
  while $[\|e\|_{x_-;\mu}] >$ DesiredAccuracy:Discretization(x) *(cf.* (25)*)*
  compute $[\Theta](x_-)$ *(cf.* (21)*)*
  compute $[\|x - x(\mu)\|_{x_-;\mu}]$ *(cf.* (30)*)*
  success = $([\|x - x(\mu)\|_{x_-;\mu}] \leq$DesiredAccuracy:Corrector$(\mu))$ *(cf.* (31)*)*
  failure = $([\Theta](x_-) >$ RequiredContraction$)$
  $x_- \leftarrow x$
while not(success $\vee$ failure)

Figure 3: Sketch of an inexact Newton corrector.

a convergent sequence of iterates. However, we are mainly interested in the error reduction of one particular Newton step, rather than in the asymptotic behavior of the iteration.

Theorem 3.3. *Let R be a linear space, X a normed space and consider $F : X \supset D \to R$. Assume there exists $x_* \in D$ with $F(x_*) = 0$. For given $x_- \in D$ assume that there exists an invertible linear mapping $F'(x_-)(\cdot) : X \to R$ such that the quantity*

$$\Theta(x) := \frac{\left\| F'(x_-)^{-1} \left[F'(x_-)(x_- - x_*) - (F(x_-) - F(x_*)) \right] \right\|}{\|x_- - x_*\|} \tag{17}$$

is well defined. Assume that an inexact Newton step with inexactness e

$$x := x_- - F'(x_-)^{-1} F(x_-) + e, \quad \Delta := \frac{\|e\|}{\|x_- - x_*\|}$$

can be performed such that

$$\Delta + \Theta(x_-) \leq \beta < 1. \tag{18}$$

Then

$$\|x - x_*\| \leq \beta \|x_- - x_*\|. \tag{19}$$

Proof. We compute for one inexact Newton step:

$$\begin{aligned} \|x - x_*\| &= \left\| x_- - F'(x_-)^{-1} F(x_-) + e - x_* \right\| \\ &\leq \left\| F'(x_-)^{-1} \left[F'(x_-)(x_- - x_*) - (F(x_-) - F(x_*)) \right] \right\| + \|e\|. \end{aligned}$$

Inserting the definition of $\Theta(x)$ and assumption (18) we obtain

$$\|x - x_*\| \leq (\Theta(x_-) + \Delta) \|x_- - x_*\| \leq \beta \|x_- - x_*\|.$$

□

Observe that the numerator of the right hand side in (17) is an affine invariant version of the remainder term of semi-smooth Newton methods (consider the term in brackets). If $\lim_{x\to x_*}\Theta(x)=0$ and $\Delta=0$, then by induction Theorem 3.3 yields the well known result of local superlinear convergence of semi-smooth Newton methods (cf. e.g. [40, 23, 29]).

This simple theorem already captures much of the algorithmic issues encountered. In particular, (18) and (19) describe the interplay between discretization error, nonlinearity, and progress of the algorithm. We observe that for mildly nonlinear problems (or close to the solution) where $\Theta(x)\ll 1$, the relative discretization error Δ dominates the left hand side in (18).

3.2 An Estimate for the Contraction

Let us now assume that Newton steps can be computed exactly, i.e. $\Delta=0$. This is true, for example, if the equation $F(x)=0$ is a finite dimensional (discretized) problem. To judge the success of a Newton step, a computable estimate for Θ as defined in (17) is desirable. Let in the following an iterate x_- be given, and let x be the result of an exact Newton step $x_-\to x$. We will now consider $\Theta(x_-)$ in more detail. Starting with (17), $F(x_*)=0$ and $x=x_- - F'(x_-)^{-1}F(x_-)$ yield

$$\begin{aligned}\Theta(x_-) &= \frac{\left\|F'(x_-)^{-1}\left[F'(x_-)(x_- - x_*)-(F(x_-)-F(x_*))\right]\right\|}{\|x_- - x_*\|}\\ &= \frac{\left\|(x_- - x_*)-F'(x_-)^{-1}(F(x_-)-F(x_*))\right\|}{\|x_- - x_*\|} = \frac{\|x-x_*\|}{\|x_- - x_*\|}.\end{aligned} \tag{20}$$

The fundamental role of $\Theta(x_-)$ for theoretical and practical aspects of Newton methods makes it desirable to estimate its size a-posteriori during the algorithm. Since x_* is unknown, the evaluation of (20) is not possible. However, if we replace x_* by the new iterate x, which is the best we can get, we can compute the estimate

$$\begin{aligned}[\Theta](x_-) &:= \frac{\left\|F'(x_-)^{-1}\left[F'(x_-)(x_- - x)-(F(x_-)-F(x))\right]\right\|}{\|x_- - x\|}\\ &= \frac{\left\|(x_- - x)-F'(x_-)^{-1}(F(x_-)-F(x))\right\|}{\|x_- - x\|} = \frac{\|x-\overline{x}\|}{\|x_- - x\|}.\end{aligned} \tag{21}$$

Here $\overline{x}$ is given by a *simplified* Newton step:

$$\overline{x} := x - F'(x_-)^{-1}F(x).$$

This is the estimate described and analyzed in [17].

The following proposition deals with the reliability of this estimate. Semi-smoothness alone is not sufficient for reliability. This corresponds to the fact that the local radius of convergence of semi-smooth Newton methods is not stable under perturbations of the problem in general.

Proposition 3.4. *Assume that the following* strong *semi-smoothness assumption holds:*

$$\lim_{x,y\to x_*}\frac{\left\|F'(y)^{-1}\left[F'(y)(x-x_*)-(F(x)-F(x_*))\right]\right\|}{\|x-x_*\|}=0. \tag{22}$$

Then

$$\lim_{x_-\to x_*}\frac{[\Theta](x_-)}{\Theta(x_-)}=1. \tag{23}$$

Proof. For a comparison of $\Theta(x_-)$ and $[\Theta](x_-)$ we introduce the auxiliary term

$$\overline{\Theta}(x_-) := \frac{\|\overline{x} - x_*\|}{\|x - x_*\|}$$

and use the inverse triangle inequality $|\,\|a\| - \|b\|\,| \le \|a \pm b\|$ to compute

$$\begin{aligned} |\,\|x - x_*\| - \|x - \overline{x}\|\,| &\le \|x_* - \overline{x}\|\,, \\ |\,\|x_- - x_*\| - \|x_- - x\|\,| &\le \|x_* - x\|\,, \end{aligned}$$

which yields

$$\begin{aligned} \|x - x_*\|\,(1 - \overline{\Theta}(x_-)) \le \|x - \overline{x}\| \le \|x - x_*\|\,(1 + \overline{\Theta}(x_-)), \\ \|x_- - x_*\|\,(1 - \Theta(x_-)) \le \|x_- - x\| \le \|x_- - x_*\|\,(1 + \Theta(x_-)). \end{aligned}$$

Combination of these inequalities yields the estimate

$$\frac{1 - \overline{\Theta}(x_-)}{1 + \Theta(x_-)} \le \frac{\|x - \overline{x}\|\,\|x_- - x_*\|}{\|x - x_-\|\,\|x - x_*\|} = \frac{[\Theta](x_-)}{\Theta(x_-)} \le \frac{1 + \overline{\Theta}(x_-)}{1 - \Theta(x_-)}.$$

If $\lim_{x_- \to x_*} \Theta(x_-) = 0$ and $\lim_{x_- \to x_*} \overline{\Theta}(x_-) = 0$, then (23) holds. The first assumption in this statement holds, if F is semi-smooth at x_*. For the second assumption, we compute

$$\overline{\Theta}(x_-) := \frac{\|\overline{x} - x_*\|}{\|x - x_*\|} = \frac{\big\|(x - x_*) - F'(x_-)^{-1}(F(x) - F(x_*))\big\|}{\|x - x_*\|},$$

thus, $\lim_{x_- \to x_*} \overline{\Theta}(x_-) = 0$ is implied by (22). □

Remark 3.5. Equation (22) can be verified, if F is continuously Fréchet differentiable near x_* (as can be shown for interior point methods), or, in the context of semi-smooth Newton methods for control constrained optimal control problems, if strict complementarity holds. Setting $y = x_*$ we observe that F must necessarily be Fréchet differentiable at x_*.

In practice, F will be a discrete (or discretized) system, and the estimator $[\Theta](x_-)$ will be computed for this discrete system of equations. In particular, the simplified Newton iterate $\overline{x}$ has to be computed on the same discretization as the ordinary Newton iterate x. Otherwise, discretization errors may perturb the estimate substantially.

3.3 Exact and Discretized Newton Steps

As already mentioned, Newton steps in function space cannot be computed exactly, but only discrete approximations are computed. We will discuss the relation between Newton steps for the equation $F(x) = 0$ with $F : X \supset D \to R$ and Newton steps for its discretization $F_h(x) = 0$ with $F_h : X_h \supset D_h \to R$, where $X_h \subset X$ and $D_h \subset D$. We do not specify the type of discretization at this point. It is sufficient to consider F_h as a perturbation of F for the following. However, we will assume that for $h_1 < h_2$, $D_{h_2} \subset D_{h_1}$. These assumptions hold, for example, in nested conformal finite element spaces.

Let x_* and $x_{*,h}$ be zeros of F and F_h, respectively. For given initial value $x_- \in D_h$ consider again the next Newton iterate

$$x := x_- - F'(x_-)^{-1} F(x_-)$$

and its discrete counterpart

$$x_h := x_- - F_h'(x_-)^{-1} F_h(x_-).$$

Then, on the one hand, Theorem 3.3 can be applied, interpreting x_h as the result of an inexact Newton step. On the other hand, just as x is the result of an an exact Newton step for the function space problem, x_h is the result of an exact Newton step for the discretized problem, and it is an interesting question to compare the progress of both steps. In particular, we want to compare the contractions

$$\Theta(x_-) := \frac{\|x - x_*\|}{\|x_- - x_*\|}, \qquad \Theta_h(x_-) := \frac{\|x_h - x_{*,h}\|}{\|x_- - x_{*,h}\|}.$$

The first quantity $\Theta(x_-)$ reflects the progress of the exact Newton step towards the solution in function space, the second $\Theta_h(x_-)$ the progress of the discrete Newton step towards the discrete approximate solution.

We will now show that under very general assumptions, $\Theta_h(x_-)$ and $\Theta(x_-)$ will be of similar size, if only h is chosen small enough.

Proposition 3.6. *Assume that $x \neq x_*$, $\lim_{h\to 0} x_h = x$, and $\lim_{h\to 0} x_{*,h} = x_*$. Then*

$$\lim_{h\to 0} \frac{\Theta_h(x_-)}{\Theta(x_-)} = 1.$$

Proof. Since $x \neq x_*$, also $x_- \neq x_*$, because x is the result of a Newton step, starting at x_-. Hence, by our assumptions, $\|x_- - x_{*,h}\|$ is bounded from below for all sufficiently small h.

We may thus compute

$$\begin{aligned}\left|\frac{\Theta_h(x_-)}{\Theta(x_-)} - 1\right| &= \left|\frac{\|x_h - x_{*,h}\|}{\|x_- - x_{*,h}\|}\frac{\|x_- - x_*\|}{\|x - x_*\|} - 1\right| \\ &= \left|\frac{\|x_h - x_{*,h}\|\,\|x_- - x_*\| - \|x_- - x_{*,h}\|\,\|x - x_*\|}{\|x_- - x_{*,h}\|\,\|x - x_*\|}\right|. \end{aligned} \tag{24}$$

For $h \to 0$ our assumptions and the triangle inequality imply $\|x_h - x_{*,h}\| \to \|x - x_*\|$ and $\|x_- - x_{*,h}\| \to \|x_- - x_*\|$, and thus the numerator in (24) converges to 0, as $h \to 0$, while the denominator remains bounded from below. □

Proposition 3.6 states that a discrete Newton step inherits the properties of its continuous counterpart, if only the mesh is sufficiently fine. So this result plays a similar role for inexact Newton methods in function space as mesh-independence results (cf. e.g. [3, 25, 43]) do for nested iteration techniques. In contrast to these results, which consider the convergence of Newton's method for a fixed, but sufficiently fine discretization, we consider the problem for a fixed Newton step and $h \to 0$. This obviously facilitates the theoretical considerations. Mesh-dependence is obviously not a difficulty in the framework of inexact Newton methods in function space.

Note that our assumptions do not directly include restrictions on the nonlinearity of the problem, such as differentiability or semi-smoothness. But, of course the nonlinearity of the problem may play a role in verifying the assumptions $x_{*,h} \to x_*$ and $x_h \to x$ for $h \to 0$.

In a practical algorithm one will refine the grid gradually (cf. Algorithm 3.2) such that $\Theta(x_-)$ and $\Theta_h(x_-)$ are always of comparable size. Proposition 3.6 shows us that by refining the grid appropriately we will inherit the convergence behavior of Newton's method for the continuous problem. Then, by (24), applied to the discrete Newton step, an estimator $[\Theta_h](x_-)$ can be computed, which is asymptotically accurate by Proposition 3.4.

3.4 An Inexact Newton Corrector for Barrier Problems

It remains to fix the details and some variations of Algorithm 3.2 in the context of our interior point algorithm. Now, the nonlinear function F depends on a parameter μ, and $F(x;\mu)$ is defined by the optimality system (10) and $F'(x;\mu)$ is given by (11). We are looking for a zero of $F(\cdot;\mu)$, that we call $x(\mu)$.

The inner adaptive refinement loop, and in particular a problem suited error estimate $[\|e\|_{x_-;\mu}]$ is described in Section 5. The refinement loop is terminated, if a fixed, user specified *relative accuracy* is reached, that is, if

$$\frac{[\|e\|_{x_-;\mu}]}{\|\delta x\|_{x_-;\mu}} \leq \Delta_{des}. \tag{25}$$

Here

$$\delta x = -F_h'(x_-;\mu)F_h(x_-;\mu) = -F'(x_-;\mu)F(x_-;\mu) + e$$

is a discretized Newton correction, or equivalently an inexact Newton correction in function space. Reasonable choices for Δ_{des} are $\Delta_{des} \in [0.1; 0.5]$.

Pointwise damping. Once e is sufficiently small, the Newton correction δx may be added to the iterate. In the context of interior point methods, however, a more efficient and robust variant is to use a pointwise modification, proposed in [39, Sec. 5]. It consists of a pointwise damping of the state correction that guarantees feasibility of the next Newton iterate y. For a given Newton correction $\delta x = (\delta y, \delta p)$ we compute the next iterate $x = (y, p)$ via $p := p_- + \delta p$, and y, such that it satisfies pointwise at every grid point:

$$\begin{aligned} y &= y_- + \delta y \quad \forall t \in \Omega : \delta y(t) \geq 0 \\ y - y_- + l'(y;\mu) - l'(y_-;\mu) &= (1 + l''(y_-;\mu))\delta y \quad \forall t \in \Omega : \delta y(t) < 0. \end{aligned} \tag{26}$$

This means that the Newton step is damped, if it approaches the lower bounds. It was shown in [39, Sec. 5] that the second equation has exactly one (strictly feasible) solution, which can be found by simple scalar root finding techniques.

The new iterate can also be written in the form

$$y(t) = \lambda(t)\delta y(t) + y_-(t),$$

with the pointwise damping factor $\lambda(t)$, computed from (26). Again, in [39, Sec. 5] it was proved that $0 < \lambda(t) \leq 1$ with $\lambda(t) \to 1$, if $\delta y(t) \to 0$.

The computation of an estimator $[\Theta]$ for the contraction is performed as above by

$$[\Theta](x_-;\mu) := \frac{\|\delta\overline{x}\|_{x_-;\mu}}{\|\delta x\|_{x_-;\mu}}. \tag{27}$$

Here $\delta\overline{x}$ is the result of a simplified Newton step:

$$\delta\overline{x} := -F_h'(x_-;\mu)F_h(x;\mu).$$

A pointwise damped version of $\delta\overline{x}$ is added to x if $[\Theta](x_-) \leq 0.25$.

A linear model for the contraction. The convergence theory in [39, Prop. 4.7] indicates that the contraction $\Theta(x_-)$ is bounded linearly by the error $\|x_- - x(\mu)\|_{x_-;\mu}$:

$$\Theta(x_-;\mu) \leq \omega(\mu) \|x_- - x(\mu)\|_{x_-;\mu}, \tag{28}$$

as long as $\|y_- - y(\mu)\|_\infty$ is sufficiently small. The quantity $\omega(\mu)$ is closely related to an affine invariant Lipschitz constant for $F'(\cdot;\mu)$, as used in [17]. For a given Newton step $x_- \to x$ this motives the introduction of the estimate

$$[\omega](\mu) := \frac{[\Theta](x_-;\mu)}{\|x - x_-\|_{x_-;\mu}}, \tag{29}$$

where the unknown solution $x(\mu)$ in (28) has been replaced by the new iterate x, the best available information. We observe that an estimate for the radius of convergence of Newton's method, given by the requirement $\Theta(x_-;\mu) \leq \beta < 1$ is given by $r = \beta/[\omega](\mu)$. We will thus use $[\omega]$ for the update of the homotopy parameter to stay inside the region of (fast) convergence. We always evaluate $[\omega]$ at the first Newton step of the corrector.

Termination. With the help of $[\Theta](x_-;\mu)$ we construct an estimate $[\|x - x(\mu)\|_{x_-;\mu}]$ for the error of the new Newton iterate $\|x - x(\mu)\|_{x_-;\mu}$. A simple computation yields:

$$\|x - x(\mu)\|_{x_-;\mu} = \Theta(x_-;\mu) \|x_- - x(\mu)\|_{x_-;\mu} \leq \Theta(x_-;\mu)(\|x_- - x\|_{x_-;\mu} + \|x - x(\mu)\|_{x_-;\mu}),$$

and hence,

$$\|x - x(\mu)\|_{x_-;\mu} \leq \frac{\Theta(x_-;\mu)}{1 - \Theta(x_-;\mu)} \|x - x_-\|_{x_-;\mu}.$$

To get an error estimate, we insert $[\Theta](x_-;\mu)$ into this inequality. Since this computation does not yet take into account discretization errors, we have to add $[\|e\|_{x_-;\mu}]$ and obtain

$$[\|x - x(\mu)\|_{x_-;\mu}] := \frac{[\Theta](x_-;\mu)}{1 - [\Theta](x_-;\mu)} \|x - x_-\|_{x_-;\mu} + [\|e\|_{x_-;\mu}]. \tag{30}$$

If $[\|x - x(\mu)\|_{x_-;\mu}]$ is below a prescribed accuracy and $[\Theta](x_-;\mu) \leq 0.5$, then the Newton corrector is terminated successfully, and a new homotopy parameter μ is chosen (cf. Section 4.3, below). If, in contrast, $[\Theta]$ is too large, e.g., $[Theta] > 0.9$, then the Newton corrector is terminated with a failure. In this case, the Newton corrector is restarted with a more conservative value of μ.

In our path-following algorithm we impose for each Newton corrector the following *relative accuracy requirement*. Let x_{start} be the starting guess of the Newton iteration, and x the current iterate. Then we terminate the corrector, if

$$[\|x - x(\mu)\|_{x_-;\mu}] \leq \Lambda_{des} \|x_{start} - x\|_{x_-;\mu}. \tag{31}$$

Reasonable choices are $\Lambda_{des} \in [0.1; 0.5]$.

Although pointwise damping steps improve the efficiency and robustness of our algorithm drastically, measures should be taken to limit their influence on the iteration. Define

$$\lambda := \frac{\|x - x_-\|_{x_-;\mu}}{\|\delta x\|_{x_-;\mu}}$$

as a measure for the effect of the pointwise damping. Our Newton iteration is terminated with a failure, if $\lambda < 0.05$, and restarted with a more conservative value of μ. Further, we impose $\lambda \geq 0.5$ as a necessary condition for successful termination.

4 Path-following in Function Space

Consider again Algorithm 2.3. After successful termination of the corrector a new value for the homotopy parameter μ has to be chosen. For a good choice, two different quantities are important. The first one, which we have discussed in the last section, is the Newton contraction Θ. It captures the nonlinearity of the homotopy subproblems and gives us an idea of the radius of convergence of Newton's method. Second, we have to estimate how the homotopy path changes, if μ is updated. Thus, what we need is an estimate for the Lipschitz constant, or the slope of the homotopy path.

With both pieces of information at hand, it is clear, qualitatively, how to steer a path-following method. We want to choose the next μ, such that our actual iterate is inside the radius of convergence of the next corrector. The higher the nonlinearity and the slope of the path, the smaller the steps, and vice versa. A quantitative realization of this strategy can, for example, be found in [17, Chap. 5], which is the basis for our strategy presented in Section 4.3. In addition to the step size selection, information on the slope of the path also yields an estimate of its remaining length and thus a termination criterion.

In finite dimensions a popular estimate for the slope of the homotopy path is computing difference quotients of the numerical solutions for different values of μ, i.e. estimates of the form:

$$\frac{\|x_{j+1} - x_j\|}{|\mu_{j+1} - \mu_j|} \approx \frac{\|x(\mu_{j+1}) - x(\mu_j)\|}{|\mu_{j+1} - \mu_j|}.$$

In our computational framework, where adaptive grid refinement is a central point, difference quotients turn out to be not robust enough, since discretization errors may perturb this estimate substantially. This is, because x_{j+1} and x_j live on different meshes.

4.1 Differentiability of the Path

An alternative to compute the slope of the central path is given by differentiating it with respect to μ. For this purpose we first have to establish differentiability of the central path $\mu \to x(\mu)$. In this context, recall our discussion on strict feasibility of the central path in Section 2.3.

Proposition 4.1. *If $x(\mu)$ is strictly feasible for all $\mu \in]0;\infty[$, then on $]0;\infty[$ the central path $\mu \to x(\mu)$ is continuously differentiable with respect to μ. Its derivative is given by*

$$x_\mu(\mu) = \frac{d}{d\mu} x(\mu) = -F'(x(\mu);\mu) F_\mu(x(\mu);\mu),$$

and admits the bound

$$\left\| \left\| \frac{d}{d\mu} x(\mu) \right\| \right\|_{x;\mu} \leq c\mu^{-1/2}. \tag{32}$$

Proof. Our proof will be facilitated by the fact that we know existence and Lipschitz continuity of the central path $x(\mu)$. Thus, we do not have to apply the implicit function theorem as an existence result. We merely have to show that appropriate remainder terms are small. We will show in the following that the mapping $\mu \to x(\mu)$ is *strongly* differentiable (cf. [33, Def. 25.10]) for every $\mu > 0$. By [33, Thm. 25.23] on an open set strong differentiability is equivalent to continuous differentiability.

To this end define the following remainder term for $\mu_0 > 0$ and $x(\mu_0)$

$$\begin{aligned} r(\mu,\nu) &:= F'(x(\mu_0);\mu_0)(x(\mu)-x(\nu)) + F_\mu(x(\mu_0);\mu_0)(\mu-\nu) \\ &= F'(x(\mu_0);\mu_0)(x(\mu)-x(\nu)) + F_\mu(x(\mu_0);\mu_0)(\mu-\nu) - (F(x(\mu);\mu) - F(x(\nu);\nu)) \\ &= \begin{pmatrix} l''(y(\mu_0);\mu_0)(y(\mu)-y(\nu)) + l'_\mu(y(\mu_0);\mu_0)(\mu-\nu) - (l'(y(\mu);\mu) - l'(y(\nu);\nu)) \\ 0 \end{pmatrix}. \end{aligned}$$

The last equality holds because of the linearity of most components of F. In particular, the second component of r vanishes completely, and the first component is the difference of functions. Observe that, in contrast to Fréchet differentiability, we have to consider "two-sided" limits $\mu, \nu \to \mu_0$ for strong differentiability.

Since the central path is strictly feasible, $l'(y;\mu)$ is continuously differentiable with respect to y and μ in an $L_\infty(\Omega) \times \mathbb{R}$ neighborhood of $(x(\mu_0);\mu_0)$. Thus, by [33, Thm. 25.23], we have strong differentiability of F at $(x(\mu_0);\mu_0)$. It follows in particular:

$$\lim_{\substack{y(\mu),y(\nu)\to y(\mu_0) \\ \mu,\nu\to\mu_0}} \frac{\|r(\mu,\nu)\|_\infty}{\|y(\mu)-y(\nu)\|_\infty + |\mu-\nu|} = 0.$$

By Lipschitz continuity of the central path $\|y(\mu)-y(\nu)\|_\infty + |\mu-\nu| \le (L(\mu_0)+1)|\mu-\nu|$ and in particular $\mu \to \mu_0$ implies $y(\mu) \to y(\mu_0)$. Thus we conclude

$$\lim_{\mu,\nu\to\mu_0} \frac{\|r(\mu,\nu)\|_\infty}{|\mu-\nu|} \le (L(\mu_0)+1) \lim_{\mu,\nu\to\mu_0} \frac{\|r(\mu,\nu)\|_\infty}{\|y(\mu)-y(\nu)\|_\infty + |\mu-\nu|} = 0. \tag{33}$$

Application of Theorem 2.2 to $F'(x(\mu_0);\mu_0)^{-1} r(\mu,\nu)$ yields:

$$\lim_{\mu,\nu\to\mu_0} \frac{\left|\left|\left|(x(\mu)-x(\nu)) + F'(x(\mu_0);\mu_0)^{-1} F_\mu(x(\mu_0);\mu_0)(\mu-\nu)\right|\right|\right|_{x(\mu_0);\mu_0}}{|\mu-\nu|} = 0,$$

and thus $x(\mu)$ is *strongly* differentiable at μ_0 with derivative

$$x_\mu(\mu_0) = -F'(x(\mu_0);\mu_0)^{-1} F_\mu(x(\mu_0);\mu_0).$$

Since μ_0 was arbitrary, [33, Thm. 25.23] shows continuous differentiability of the central path.

Equation (32) follows straightforwardly from the computation

$$\begin{aligned} \langle b'_\mu(y;\mu), v\rangle &= c\langle \mu^{q-1} y^{-q}, v\rangle = c\mu^{-1/2}\langle (\mu/y)^{(q-1)/2}, \mu^{q/2} y^{-(q+1)/2} v\rangle \\ &= c\mu^{-1/2}\langle (\mu/y)^{(q-1)/2}, \sqrt{l''(y;\mu)}\, v\rangle \le c\mu^{-1/2} \left\|(\mu/y)^{q-1}\right\|_{L_1}^{1/2} \|(v,0)\|_{x;\mu} \end{aligned}$$

and application of Theorem 2.2, since $\left\|(\mu/y)^{q-1}\right\|_{L_1}$ is uniformly bounded, as $\mu \to 0$ (cf. [37, Cor. 4.6]). □

Remark 4.2. Since all involved quantities are smooth inside the feasible domain, it can be shown with some more technical and notational effort that the central path is C^∞ for $\mu \in]0;\infty[$, of course, with rapidly increasing derivatives as $\mu \to 0$.

By the fundamental theorem of calculus we compute

$$x(\mu_0) - x_{opt} = \lim_{\underline{\mu}\to 0} \int_{\underline{\mu}}^{\mu_0} x_\mu(\mu)\, d\mu,$$

which, together with (32) suggests the following estimate for the remaining length of the central path:

$$[\|x(\mu_0) - x_{opt}\|] := 2\mu_0 \|x_\mu(\mu_0)\|.$$

Similarly, an estimate for the error in the functional $J(x) := J(y, \alpha^{-1}B^*p)$ can be computed via

$$J(x(\mu_0)) - J(x_{opt}) = \lim_{\underline{\mu}\to 0} \int_{\underline{\mu}}^{\mu_0} \langle J_x(x(\mu)), x_\mu(\mu)\rangle \, d\mu.$$

This yields the estimate

$$[J(x(\mu_0)) - J(x_{opt})] := \mu_0 \langle J_x(x(\mu_0)), x_\mu(\mu_0)\rangle.$$

Both estimates can be used as a termination criterion, according to the needs of the user.

4.2 Inexact Evaluation

Since $x(\mu)$ cannot be computed exactly, we cannot expect to be able to evaluate $x_\mu(\mu)$ exactly. Rather, we will compute an inexact quantity of the form

$$[x_\mu](\mu) := -F'(x;\mu)^{-1} F_\mu(x;\mu). \tag{34}$$

If x is close to $x(\mu)$, we expect to obtain $x_\mu(\mu) \approx [x_\mu](\mu)$. The aim of this section is to make these considerations concrete.

Proposition 4.3. *If $\|y(\mu) - y\|_\infty$ is sufficiently small, then*

$$\|\|x_\mu(\mu) - [x_\mu](\mu)\|\|_{x(\mu);\mu} \le C \left(\mu^{-1} + \left\|(y(\mu) - \underline{y})^{-1}\right\|_\infty \|[x_\mu](\mu)\|_{x(\mu);\mu}\right) \|x(\mu) - x\|_{x(\mu);\mu}.$$

In particular, if $\|x(\mu) - x\|_{x(\mu);\mu} \to 0$, then also $\|\|x_\mu(\mu) - [x_\mu](\mu)\|\|_{x(\mu);\mu} \to 0$.

Proof. Since we keep μ fixed, we abbreviate $F(\cdot;\mu)$ by $F(\cdot)$, and so on. Further, set $\underline{y} = 0$, w.l.o.g.. Let $\hat{x} = (\hat{y}, \hat{p})$ with $\hat{y}$ strictly feasible and y be close to $\hat{y}$, such that $\rho_1 y \le \hat{y} \le \rho_2 y$ for some $0 < \rho_1 < 1 < \rho_2$.

$$\begin{aligned} &F'(\hat{x})^{-1}F_\mu(\hat{x}) - F'(x)^{-1}F_\mu(x) \\ &\qquad = F'(\hat{x})^{-1}\left(F_\mu(\hat{x}) - F_\mu(x)\right) - F'(\hat{x})^{-1}\left(F'(\hat{x}) - F'(x)\right)F'(x)^{-1}F_\mu(x). \end{aligned} \tag{35}$$

Here, the following differences can be computed as pointwise relations:

$$\begin{aligned} (F_\mu(\hat{x}) - F_\mu(x))(t) &= l'_\mu(\hat{y}(t)) - l'_\mu(y(t)) \\ ((F'(\hat{x}) - F'(x))\delta x)(t) &= (l''(\hat{y}(t)) - l''(y(t)))\delta y(t). \end{aligned}$$

Note that the second rows of F_μ and $F'(\hat{x}) - F'(x)$ are zero, and have thus been left away. Since l'' and l'_μ are rational functions and thus continuously differentiable on $]0;\infty[$, we compute pointwise for some $\bar{y}, \tilde{y} \in [\rho_1 y; \rho_2 y]$:

$$\begin{aligned} l'_\mu(\hat{y}) - l'_\mu(y) &= l''_\mu(\bar{y})(\hat{y} - y) \le C\mu^{-1} l''(\hat{y})(\hat{y} - y) \\ l''(\hat{y}) - l''(y) &= l'''(\tilde{y})(\hat{y} - y) \le C\hat{y}^{-1} l''(\hat{y})(\hat{y} - y). \end{aligned}$$

Here C depends on ρ_1, ρ_2 and the order of the barrier functional q only. Application of Theorem 2.2 yields

$$\begin{aligned}\left|\left|\left|F'(\hat{x})^{-1}(F_\mu(\hat{x})-F_\mu(x))\right|\right|\right|_{\hat{x};\mu} &\leq C\mu^{-1}\sup_{v\in Y}\frac{\langle l''(\hat{y})(\hat{y}-y),v\rangle}{|||(v,0)|||_{\hat{x};\mu}}\\ &\leq \sup_{v\in Y}\frac{\|(\hat{y}-y,0)\|_{\hat{x};\mu}\,\|(v,0)\|_{\hat{x};\mu}}{|||(v,0)|||_{\hat{x};\mu}} \leq C\mu^{-1}\left\|\hat{x}-x\right\|_{\hat{x};\mu}.\end{aligned}$$

Similarly, denoting by $[y_\mu]$ the first component of $-F'(x)^{-1}F_\mu(x)$

$$\begin{aligned}\left|\left|\left|-F'(\hat{x})^{-1}((F'(\hat{x})-F'(x))F'(x)^{-1}F_\mu(x)\right|\right|\right|_{\hat{x};\mu} &\leq C\sup_{v\in Y}\frac{\langle\hat{y}^{-1}l''(\hat{y})(\hat{y}-y)[y_\mu],v\rangle}{|||(v,0)|||_{x;\mu}}\\ \leq C\sup_{v\in Y}\frac{\left\|\hat{y}^{-1}l''(\hat{y})(\hat{y}-y)[y_\mu]\right\|_{L_1}\|v\|_\infty}{|||(v,0)|||_{\hat{x};\mu}} &\leq C\left\|\hat{y}^{-1}\right\|_\infty\|(\hat{x}-x)\|_{\hat{x};\mu}\,\|[x_\mu]\|_{\hat{x};\mu}.\end{aligned}$$

Now, application of the triangle inequality to (35) yields the desired result, when we set $\hat{x}=x(\mu)$. □

This proposition asserts that the slope of the interior point homotopy path can be evaluated to a certain accuracy, in a neighborhood of $x(\mu)$. Comparison with the convergence results in [39] indicates that the size of this neighborhood corresponds to the size of the region of Newton contraction. Hence, we may expect accurate slope information at the solution of the Newton corrector.

Applicability of similar estimates to path-following methods with only semi-smooth equations appears questionable, since continuity of the Jacobian matrix is not guaranteed in this case. This is reflected by the observation that those homotopy paths are usually not continuously differentiable, but only locally Lipschitz continuous.

4.3 Update of the Homotopy Parameter

Assume that the Newton corrector has finished successfully for some μ_j. Then, equipped with the quantities $[x_\mu](\mu_j)$ from (34), $[\omega](\mu_j)$ from (29), and $[\|x-x(\mu)\|_{x;\mu}]$ from (30), we can construct a heuristic to update μ_{j+1} for the homotopy parameter. For a given iterate x_j, we would like to choose a new homotopy parameter μ_{j+1}, such that

$$\omega(\mu_{j+1})\left\|x_j-x(\mu_{j+1})\right\|_{x_j;\mu_{j+1}} \approx \Theta_{des}, \tag{36}$$

where Θ_{des} is a user provided *desired contraction*. Reasonable values are $\Theta_{des}\in[0.1;0.75]$.

Under the assumption $\omega(\mu)\approx O(\mu^{-1/2})$ (which is reasonable from numerical experience) we introduce the model

$$[\omega(\mu)] := [\omega](\mu_j)\sqrt{\frac{\mu_j}{\mu}}. \tag{37}$$

Further, the triangle inequality yields

$$\left\|x_j-x(\mu_{j+1})\right\|_{x_j;\mu_j} \leq \left\|x_j-x(\mu_j)\right\|_{x_j;\mu_j} + \left\|x(\mu_j)-x(\mu_{j+1})\right\|_{x_j;\mu_j}.$$

For the first term in the right hand side an estimate $[\|x_j-x(\mu_j)\|_{x_j;\mu_j}]$ is given by (30), while the second term can be computed via

$$\left\|x(\mu_j)-x(\mu_{j+1})\right\|_{x_j;\mu_j} \leq \int_{\mu_{j+1}}^{\mu_j}\left\|x_\mu(\mu)\right\|_{x_j;\mu_j}\,d\mu.$$

For the integrand we insert our estimate (34) and the model (cf. (32)):

$$[\|x_\mu(\mu)\|_{x_j;\mu_j}] := \|[x_\mu](\mu_j)\|_{x_j;\mu_j} \sqrt{\frac{\mu_j}{\mu}}.$$

Then

$$\begin{aligned}\int_{\mu_{j+1}}^{\mu_j} \|x_\mu(\mu)\|_{x_j;\mu_j}\, d\mu &\approx \int_{\mu_{j+1}}^{\mu_j} \|[x_\mu](\mu_j)\|_{x_j;\mu_j} \sqrt{\frac{\mu_j}{\mu}}\, d\mu \\ &= \|[x_\mu](\mu_j)\|_{x_j;\mu_j}\, 2\sqrt{\mu_j}(\sqrt{\mu_j} - \sqrt{\mu_{j+1}}).\end{aligned} \tag{38}$$

Now we choose the next homotopy parameter as follows:

$$\mu_{j+1} := \sigma\mu_j,$$

where the step size (or μ-reduction factor) $\sigma \in]0;1[$ is computed to satisfy:

$$[\omega](\mu_j)\sigma^{-1/2}\left([\|x_j - x(\mu)\|_{x_j;\mu_j}] + \|[x_\mu](\mu_j)\|_{x_j;\mu_j}\, 2\mu_j(1-\sqrt{\sigma})\right) = \Theta_{des}.$$

Observe that the left hand side of this equation is an estimate for the left hand side of (36), using (29), (37), (30), (34), and (38). Here we have ignored the dependence of our norm $\|\cdot\|_{x;\mu}$ on x and μ. This can also be taken into account (cf. [42]).

In the context of adaptive grid refinement, too aggressive choices of σ are not useful, because the grid refinement procedure necessitates a couple of iterations anyway. So we restrict the choice of σ to $\sigma \geq 1/16$, which corresponds to a reduction of the homotopy error by 1/4 (cf. (8)). This is the maximal error reduction in the L_2-norm that can be obtained by one refinement step with linear finite elements.

If the Newton corrector has failed, for example, if $[\Theta] \gg \Theta_{des}$ then we have to recompute μ_j, using again $[\Theta]$ from the failed corrector step to update $[\omega]$. We obtain a similar step size rule as just described, which will yield a more conservative value of σ, and thus μ_j as in the failed step. Details can be found in [39, Sec. 6].

Remark 4.4. In the presence of tangent information, it is an obvious idea to use an approximate tangential predictor for the path-following method. This idea has several variants of implementation, and there is some care necessary in providing algorithmic details. Also, the numerical examples at the end of this paper indicate that a further improvement in this direction will not yield significant gains in efficiency. Thus, we do not pursue this idea in our present work.

5 Discretization Error Analysis

Our previous considerations were all based on the assumption that it is possible to control the discretization error efficiently. We will now propose a method to achieve this goal with reasonable computational effort by using specially constructed a-posteriori error estimates. Their most interesting feature is that they yield error estimators and indicators for the norm that governs our algorithm in function space, namely the norm $\|\cdot\|_{x;\mu}$. They can be deduced via a simple orthogonality argument, and their implementation resembles strongly the well established dual weighed residual error estimates [7].

Remark 5.1. In [45] classical goal-oriented error estimators were proposed in the context of interior point methods for the error in the functional $J(\cdot) + b(\cdot;\mu)$. These estimators are

motivated by the experience that users often wish to obtain an accurate approximation of J with small computational effort. In contrast, the construction of our estimator is motivated by the convergence analysis of our path-following algorithm. Since both estimators require similar computations, one may think of combining both ideas in one method.

Consider for fixed μ the structure of the Jacobian matrix (11) of (10). It is easy to see that it is decomposed into a symmetric positive definite part and a skew-symmetric part:

$$F'(x;\mu) = \begin{pmatrix} I + b''(y;\mu) & 0 \\ 0 & \alpha^{-1}BB^* \end{pmatrix} + \begin{pmatrix} 0 & A^* \\ -A & 0 \end{pmatrix}, \tag{39}$$

and that the symmetric part induces the natural norm $\|\cdot\|_{x;\mu}$. This motivates the following considerations.

5.1 Sums of Monotone and Skew-Symmetric Operators

Let $T(\cdot) = S(\cdot) + H(\cdot) : X \supset D \to X^*$ be some nonlinear mapping, and assume that H is skew-symmetric, i.e.

$$\langle H(v) - H(w), v - w\rangle = 0. \tag{40}$$

Let X_h be a closed subspace of X (usually X_h is a finite element subspace). We assume that there exist $x \in X$, $x_h \in X_h$, and $x^h \in X_h$ that solve the following equations:

$$T(x) = 0 \quad \text{in } X^*, \tag{41}$$

$$\langle T(x_h), v_h\rangle = 0 \quad \forall v_h \in X_h, \tag{42}$$

$$\langle H(x) - H(x^h), v_h\rangle = 0 \quad \forall v_h \in X_h. \tag{43}$$

Lemma 5.2. *With the above definitions and assumptions we have*

$$\langle S(x) - S(x_h), x - x_h\rangle = -\langle T(x_h), x - v_h\rangle \quad \forall v_h \in X_h \tag{44}$$

$$\langle S(x) - S(x_h), x_h - x^h\rangle = 0. \tag{45}$$

Proof. We use (41) to compute

$$S(x) - S(x_h) = T(x) - H(x) - T(x_h) + H(x_h) = H(x_h) - H(x) - T(x_h). \tag{46}$$

Testing this equation with $v = x - x_h$ yields $\langle H(x_h) - H(x), x - x_h\rangle = 0$ and thus

$$\langle S(x) - S(x_h), x - x_h\rangle = -\langle T(x_h), x - x_h\rangle.$$

Now (44) follows, because by (42) $\langle T(x_h), v_h - x_h\rangle = 0$ for all $v_h \in X_h$.

Testing (46) with $v_h = x_h - x^h$ yields due to (42), (40) and (43)

$$\begin{aligned}\langle S(x) - S(x_h), x_h - x^h\rangle &= \langle H(x_h) - H(x), x_h - x^h\rangle - \langle T(x_h), v_h\rangle \\ &= \langle H(x_h) - H(x^h), x_h - x^h\rangle + \langle H(x^h) - H(x), x_h - x^h\rangle = 0.\end{aligned}$$

□

Assume that for each $v, w \in X$ there is a linear symmetric positive definite $\tilde{S}(v,w) \in L(X, X^*)$ that satisfies $\tilde{S}(v,w)(v-w) = S(v) - S(w)$. Then

$$\langle y, z\rangle_S := \left\langle \tilde{S}(v,w)(y), z \right\rangle \tag{47}$$

defines a positive definite bilinear form, and $\|v\|_S := \sqrt{\langle v, v\rangle_S}$ is a norm.

Corollary 5.3. *Under the above assumptions we have*

$$\|x - x_h\|_S^2 = -\langle T(x_h), x - v_h\rangle \quad \forall v_h \in X_h, \tag{48}$$

$$\|x - x_h\|_S^2 + \|x_h - x^h\|_S^2 = \|x - x^h\|_S^2 . \tag{49}$$

Proof. Since $\langle x - x_h, v\rangle_S = \langle S(x) - S(x_h), v\rangle$, (48) follows from (44) and (49) follows from (45) and the theorem of Pythagoras. □

Example: an affine case. If $S : x \to \tilde{S}x + r$, where $r \in X^*$, is an affine mapping with $\tilde{S}$ symmetric positive definite, then

$$\langle v, w\rangle_S = \left\langle \tilde{S}v, w \right\rangle \tag{50}$$

satisfies all our assumptions, since $S(v) - S(w) = \tilde{S}(v - w)$.

Remark 5.4. Although in this paper we consider only the case of an affine operator S, we remark that in a couple of applications a nonlinear operator S may appear. For example, control constrained problems can be treated by the use of a nonlinear S.

5.2 Application to Interior Point Methods

Our abstract results are readily applied to the discretization of Newton steps from interior point methods. For this recall the notation of Section 3, and let $x^h = (y^h, p^h)$, where y^h and p^h are the Galerkin approximations of y w.r.t. A and p w.r.t. A^*, respectively.

Theorem 5.5. *Consider a Newton step $x_- \to x$ for the solution of* (10) *and its discrete version $x_- \to x_h$. Then the following error estimate holds:*

$$\|x - x_h\|_{x_-;\mu} \le \|x - x^h\|_{x_-;\mu} \le C(\mu)\, \|x - x^h\|_{L_2} . \tag{51}$$

Moreover, we have the following a-posteriori error representation:

$$\|x - x_h\|_{x_-;\mu}^2 = -\langle \rho_1, y - v_h\rangle - \langle \rho_2, p - w_h\rangle \tag{52}$$

with arbitrary $(v_h, w_h) \in X_h$ and

$$\rho_1 := (I + b''(y_-;\mu))y_h + A^* p_h - y_d + b'(y_-;\mu) - b''(y_-;\mu)y_- \tag{53}$$

$$\rho_2 := -Ay_h + \alpha^{-1} BB^* p_h. \tag{54}$$

Proof. One Newton step can be written as

$$\begin{aligned}(I + b''(y_-;\mu))(y - y_-) + A^*(p - p_-) + y_- - y_d + b'(y_-;\mu) + A^* p_- = 0\\ -A(y - y_-) + \alpha^{-1} BB^*(p - p_-) - Ay_- + \alpha^{-1} BB^* p_- = 0\end{aligned}$$

or equivalently

$$\begin{aligned}(I + b''(y_-;\mu))y - y_d + b'(y_-;\mu) - b''(y_-;\mu)y_- + A^* p = 0\\ \alpha^{-1} BB^* p - Ay = 0.\end{aligned}$$

This yields our definition of $T(x)$, and we set

$$H(x) := \begin{pmatrix} A^* p \\ -Ay \end{pmatrix},$$

which is skew-symmetric and $S(x) = T(x) - H(x)$. We compute

$$S(x) - S(x_h) = \begin{pmatrix} (I + b''(y_-;\mu))(y - y_h) \\ \alpha^{-1} BB^*(p - p_h) \end{pmatrix}.$$

Now (51) is a consequence of (49) and (52) follows from (48). □

The point of the error representation (52) is that we obtain an error estimator for the natural norm (12) which – as described above – governs the convergence of Newton's method, and which is also used for the construction of the contraction estimates $[\Theta](x_-)$ in (21). It can thus be used to produce triangulations that yield small discretization errors with respect to the natural norm. This helps to bridge the gap between function space analysis and discrete implementation.

5.3 Practical Error Estimation

We return now to our concrete example of optimal control problems subject to an elliptic partial differential equation.

For the implementation of an a-posteriori error estimator on the base of (52) we may use well known techniques from goal oriented error estimation. The main issues are finding an appropriate representation of the terms $y - v_h$ and $p - w_h$ in (52) and construction of error indicators, i.e. localization of (52) onto the cells of the triangulation. Therefor a couple of heuristic techniques are available. A popular technique is to interpolate the discrete solutions y_h and p_h by polynomials of higher order on each cell and its neighbors (cf. [21]). This technique has proved effective for large classes of problems. It may, however, have difficulties with problems with jumping coefficients. Usually the jumps in the coefficients are aligned along the grid, and the gradient of the exact solution has a jump along the boundary and violate the smoothness assumptions implicitely imposed by the interpolation process. Therefore our error representation uses a technique that is based on the implicit error estimates of Bank and Weiser [5]. This means, we solve local Neumann problems on each cell within a locally finer space compared to X_h. We construct our error estimators along the lines of [1, Sec. 3.3].

In order to proceed we need some notation. Let us introduce for a polygonal, open and bounded domain $\Omega \subset \mathbb{R}^d$ ($d \in \{1, 2, 3\}$) an affine, simplicial mesh $\mathcal{T}$ consisting of a finite number of simplices T in $\mathbb{R}^d$ forming an admissible partition of Ω. Let us further define the set of all faces $\mathcal{F} := \cup_{T\in\mathcal{T}} \partial T$ and the maximum mesh size $h := \max_{T\in\mathcal{T}} \operatorname{diam}(T)$. For one single cell $T \in \mathcal{T}$ we additionally introduce the set $\mathcal{F}_T := \partial T$ and its unit outward normals n_f for $f \in \mathcal{F}_T$. Now for a given mesh or triangulation $\mathcal{T}$ we fix the finite dimensional subspace of $W^{1,\infty}(\Omega)$

$$Z_h := \{z_h \in C^0(\overline{\Omega}) : z_h \text{ is a linear polynomial on each } T \in \mathcal{T}\}$$

and define X_h as a subspace of $X = Y \times P$ to be $X_h := Z_h \times Z_h$.

So the components of our solution $x_h = (y_h, p_h) \in X_h$ are piecewise affine linear on each cell T. As already announced we are looking for approximations for y and p within a locally enriched space. For $T \in \mathcal{T}$ our choice falls onto the space of all quadratic polynomials over T denoted by S_T. Since we are going to solve local Neumann problems, we restrict this space to all functions with vanishing integral to retain unique solvability of these problems. Our definition is thus:

$$S_T = \left\{ v_h \text{ is a quadratic polynomial on } T : \int_T v_h \, dt = 0 \right\}.$$

Error representations. We will replace the unknown arguments $y - v_h$ and $p - w_h$ in (52) by e_y and $e_p \in S_{\mathcal{T}} := \prod_{T\in\mathcal{T}} S_T$ which solve local Neumann problems on each cell we still have to state. For that we need the bilinear form $a : H^1(\Omega) \times H^1(\Omega) \to \mathbb{R}$ given by $a(v,w) = \langle Av, w\rangle = \int_\Omega \langle \kappa\nabla v, \nabla w\rangle + avw\,dt$ and its restriction onto a cell $T \in \mathcal{T}$ given by

$$a_T(v,w) = \int_T \langle \kappa\nabla v, \nabla w\rangle + avw\,dt.$$

Further, we define the "averaged normal gradients" of a function $z_h \in Z_h$ and their modifications on the boundary by

$$\left\langle \frac{\partial z_h}{\partial n_f} \right\rangle_\kappa := \begin{cases} \frac{1}{2} n_f \cdot ((\kappa\nabla z_h)_T + (\kappa\nabla z_h)_{T'}) & : \quad f = \overline{T} \cap \overline{T'} \\ n_f \cdot (\kappa\nabla z_h)_T & : \quad f = \overline{T} \cap \Gamma_D \\ g & : \quad f = \overline{T} \cap \Gamma_N. \end{cases}$$

Here we included the possibility of mixed boundary conditions: Γ_D is the part of the boundary, where Dirichlet conditions holds, while Γ_N is the part of the boundary, where the Neumann condition $n_f \cdot \kappa\nabla y = g$ holds.

Note that $\kappa\nabla z_h$ is a function, defined on each $T \in \mathcal{T}$, and may have jumps at the element faces. We denote by $(\kappa\nabla z_h)_T$ its continuous extension from T to $\overline{T}$.

For efficiency of computation we only capture the "leading" terms introduced by the boundary jumps. This means, we solve the two decoupled problems: Find $e_{y|T}, e_{p|T} \in S_T$ such that

$$a_T(e_{y|T}, v) = -a_T(y_h, v) + \sum_{f\in\mathcal{F}_T} \int_f \left\langle \frac{\partial y_h}{\partial n_f} \right\rangle_\kappa v\,ds$$

$$a_T(w, e_{p|T}) = -a_T(w, p_h) + \sum_{f\in\mathcal{F}_T} \int_f \left\langle \frac{\partial p_h}{\partial n_f} \right\rangle_{\kappa^T} w\,ds$$

for all $v, w \in S_T$ and all $T \in \mathcal{T}$.

Having at hand e_y and e_p we end up with a computable error representation of (52) as

$$\|x - x_h\|^2_{x_-;\mu} \approx -\langle \rho_1, e_y\rangle - \langle \rho_2, e_p\rangle. \tag{55}$$

Evaluation of the residuals and error indicators. The L_2-part of (55) is evaluated straightforwardly

$$\langle \rho_1^0, e_y\rangle_T := \int_T ((I + b''(y_-;\mu))y_h - y_d + b'(y_-;\mu) - b''(y_-;\mu)y_-)\, e_y\,dt \tag{56}$$

$$\langle \rho_2^0, e_p\rangle_T := \int_T \alpha^{-1} B^* p_h B^* e_p\,dt. \tag{57}$$

Here (57) is used in the case of distributed control $B^* = Id$. In Neumann boundary control B^* is the trace operator, so (57) is defined by evaluation of integrals on the boundary.

It remains to evaluate the differential parts $\langle A^* p_h, e_y\rangle$ and $\langle Ay_h, e_p\rangle$. For these we use partial integration on the cells of the triangulation so that the differential operator in the weak form is replaced by the strong form and jump terms along the boundaries of the cells appear. This technique is standard in goal oriented error estimation. In our case partial integration yields the following strong residuals

$$\langle Ay_h, e_p\rangle_T = \int_T -\mathrm{div}(\kappa\nabla y_h)e_p + ay_h e_p\,dt + \sum_{f\in\mathcal{F}_T} \int_f \left[\frac{\partial y_h}{\partial n_f}\right]_\kappa e_p\,ds,$$

where:

$$\left[\frac{\partial z_h}{\partial n_f}\right]_\kappa := \begin{cases} \frac{1}{2} n_f \cdot ((\kappa \nabla z_h)_T - (\kappa \nabla z_h)_{T'}) & : \quad f = \overline{T} \cap \overline{T'} \\ 0 & : \quad f = \overline{T} \cap \Gamma_D \\ n_f \cdot (\kappa \nabla z_h)_T - g & : \quad f = \overline{T} \cap \Gamma_N. \end{cases}$$

Similarly, for the adjoint operator

$$\langle A^* p_h, e_y \rangle_T = \int_T -\mathrm{div}(\kappa^T \nabla p_h) e_y + a p_h e_y \, dt + \sum_{f \in \mathcal{F}_T} \int_f \left[\frac{\partial p_h}{\partial n_f}\right]_{\kappa^T} e_y \, ds.$$

Partial integration is a well known technique in DWR-methods ([8]). It decouples the error estimates on the grid cells and thus avoids oscillatory behavior of the error indicators.

Finally, for the evaluation of $\langle \rho_1, e_y \rangle$ and $\langle \rho_2, e_p \rangle$, the L_2-parts and the differential parts are added. Error indicators are thus computed by:

$$\eta_T := -\langle \rho_1^0, e_y \rangle_T - \langle A^* p_h, e_y \rangle_T - \langle \rho_2^0, e_p \rangle_T + \langle A y_h, e_p \rangle_T,$$

The overall residual can now be evaluated by adding all indicators (cf. (52))

$$[\|x - x_h\|^2_{x_-;\mu}] = [\|e\|_{x_-;\mu}] := -\langle \rho_1, e_y \rangle - \langle \rho_2, e_p \rangle = \sum_{T \in \mathcal{T}} \eta_T \tag{58}$$

and elements are marked for refinement if $|\eta_T|$ is large. In our particular implementation we use a so called "bulk"-criterion, where one looks for a subset $\mathcal{M} \subset \mathcal{T}$, as small as possible, such that

$$\sum_{T \in \mathcal{M}} |\eta_T| \leq \beta \sum_{T \in \mathcal{T}} |\eta_T| \quad \text{for given } 0 < \beta < 1.$$

In view of the accuracy requirement (25) imposed on the Newton step, we choose

$$\beta := \max\left\{0.2, \min\left\{0.8, \sqrt{1-\gamma^2}\right\}\right\} \text{ where } \gamma := \min\left\{1, \frac{\delta}{|[\|e\|_{x_-;\mu}]| / \|x_- - x\|_{x_-;\mu}}\right\}.$$

Consequently, many cells are refined, if the required relative accuracy is much smaller than the estimated relative accuracy. Otherwise, fewer cells are refined.

Direct evaluation of the scaled norm. For an error estimate, we may of course compute the scaled norm of our error representations $\|(e_y, e_p)\|^2_{x_-;\mu}$. Since we know

$$-\langle \rho_1, y - y_h \rangle - \langle \rho_2, p - p_h \rangle = \|x - x_h\|^2_{x_-;\mu},$$

we expect to obtain

$$-\langle \rho_1, e_y \rangle - \langle \rho_2, e_p \rangle \approx \|(e_y, e_p)\|^2_{x_-;\mu}. \tag{59}$$

A computational comparison of both quantities yields a rough, inexpensive assessment of the quality of e_y and e_p. In practice, it turns out that for the overall error, the right hand side of (59) is a more stable criterion, since it consists of a sum of positive numbers on each triangle. In contrast, the left hand side consists of two components, which can be expected to be larger in absolute value than their sum, and thus cancellation effects can spoil the overall estimate.

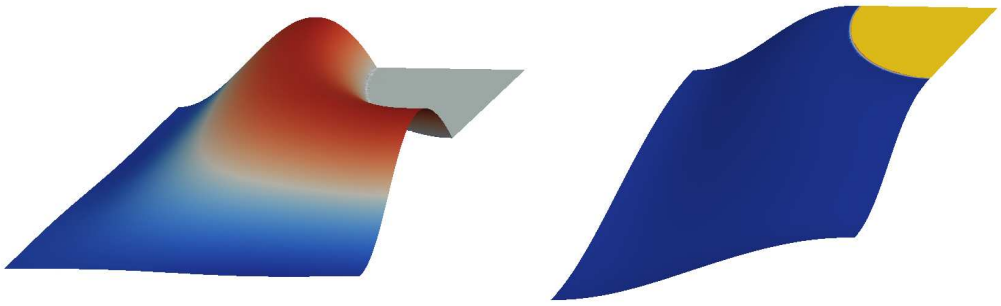

Figure 4: Neumann problem. Left: optimal control. Right: optimal state with active set.

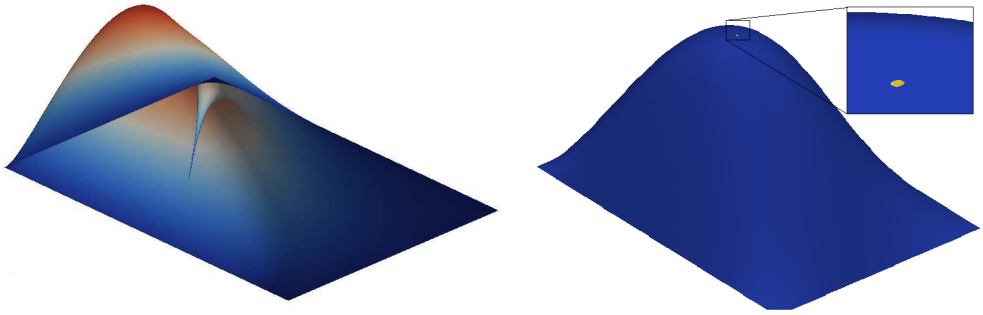

Figure 5: Dirichlet problem. Left: optimal control. Right: optimal state with (very small) active set.

6 Numerical Experiments

We have implemented an interior point path-following algorithm along the lines of the preceeding sections. The implementation was based on the KASKADE 7 library from the Zuse Institute Berlin, which in turn builds upon the DUNE library [6]. The linear systems of equations, which arise from the discretization of the Newton steps with linear finite elements, were solved by the direct sparse solver PARDISO [34].

To assess the numerical performance of our method, we consider the following simple numerical example in two variants. We choose $\Omega =]0;1[\times]0;1[$ and a state equation of the form

$$\int_\Omega \langle \nabla y, \nabla w \rangle + yw - uw \, dt = 0.$$

This is a distributed control problem. Further we choose an upper bound $\overline{y} = 0.55$, a control cost $\alpha = 10^{-3}$, and a desired state $y_d := 2 \cdot t_1 \cdot t_2$. As boundary conditions we use homogenous Dirichlet conditions as the first variant, and homogenous Neumann conditions as the second variant. The upper bound $\overline{y}$ is chosen such that in the Dirichlet case there is an extremely small active set, while in the Neumann case the active set is relatively large (see Figures 4 and 5, respectively). For these examples, no analytic solution is available, thus, all following error measurements are computed, using a more accurate solution.

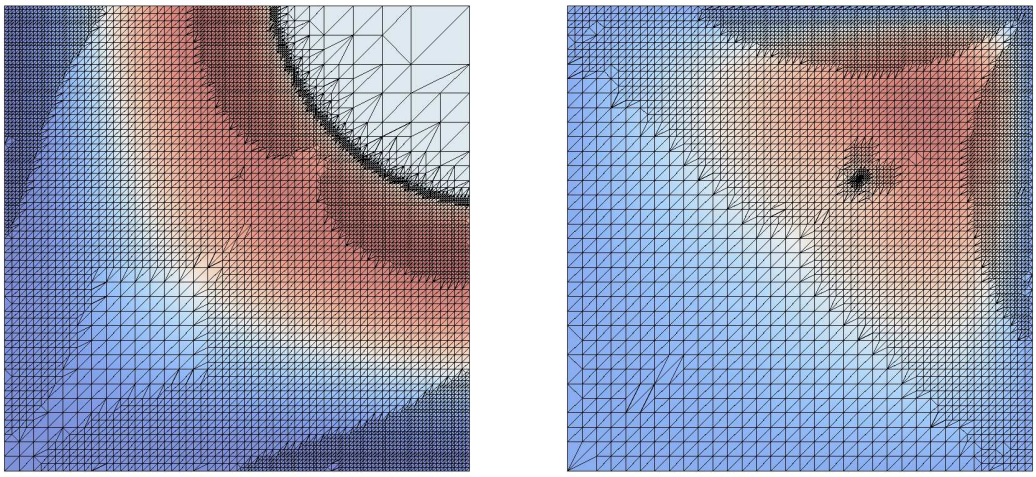

Figure 6: Computational grids for both problems, near $\mu = 10^{-6}$.

	$\mu \approx 10^{-2}$			$\mu \approx 10^{-4}$			$\mu \approx 10^{-6}$		
step	n_Δ	e_{meas}	*eff*	n_Δ	e_{meas}	*eff*	n_Δ	e_{meas}	*eff*
1	139	$8.1 \cdot 10^{-3}$	0.76	1361	$1.4 \cdot 10^{-3}$	0.87	23k	$1.1 \cdot 10^{-4}$	0.86
2	327	$5.6 \cdot 10^{-3}$	0.61	3036	$6.5 \cdot 10^{-4}$	0.83	48k	$5.3 \cdot 10^{-5}$	0.73
3	730	$2.1 \cdot 10^{-3}$	0.74	6557	$3.5 \cdot 10^{-4}$	0.74	103k	$2.6 \cdot 10^{-5}$	0.68
4	1541	$9.4 \cdot 10^{-4}$	0.70	15k	$1.5 \cdot 10^{-4}$	0.76	226k	$1.2 \cdot 10^{-5}$	0.71
	$\mu \approx 10^{-2}$			$\mu \approx 10^{-4}$			$\mu \approx 10^{-6}$		
step	n_Δ	e_{meas}	*eff*	n_Δ	e_{meas}	*eff*	n_Δ	e_{meas}	*eff*
1	456	$6.5 \cdot 10^{-3}$	0.81	2046	$1.7 \cdot 10^{-3}$	1.1	9033	$4.0 \cdot 10^{-4}$	1.1
2	878	$3.3 \cdot 10^{-3}$	0.86	4415	$9.5 \cdot 10^{-4}$	0.83	20k	$1.8 \cdot 10^{-4}$	0.88
3	2051	$1.5 \cdot 10^{-3}$	0.83	9097	$4.8 \cdot 10^{-4}$	0.79	42k	$8.2 \cdot 10^{-5}$	0.8
4	4143	$7.7 \cdot 10^{-4}$	0.89	20k	$2.0 \cdot 10^{-4}$	0.84	97k	$3.9 \cdot 10^{-5}$	0.73

Figure 7: Error estimators for the Neumann problem (top) and the Dirichlet problem (bottom).

6.1 Performance of the Error Estimators

To obtain an impression of the performance of the a-posteriori error estimators we exemplary compute some Newton steps as they may appear during the run-time of the homotopy method with adaptive refinement. For this we stopped the homotopy at various values of μ and performed one Newton step to high accuracy at this point. The tables in Figure 7 document the first four steps of this refinement process, in Figure 6 two typical grids are printed. In all cases we have listed the number of triangles n_Δ, the natural norm $\|\cdot\|_{x;\mu}$ of the discretization error e_{meas} (obtained by comparison with a much more accurate solution), and the efficiency of the estimator *eff*, given by the quotient of the estimated error and the measured error. We observe a reasonable performance in all cases. This is certainly also due to the fact that the refinement process has already started on a well adapted grid, created by the preceeding homotopy steps. Also, it can be observed that the discretization error e_{meas} is roughly proportional to n_Δ^{-1}.

e_{des}	e_{meas}	$J_{final} - J_{acc}$	T_{total}	T_{hom}	n_Δ	μ_{final}	n_{hom}
10^{-2}	$0.7 \cdot 10^{-2}$	$3.2 \cdot 10^{-4}$	2.1s	1.9s	720	$3.2 \cdot 10^{-4}$	16
10^{-3}	$0.7 \cdot 10^{-3}$	$3.1 \cdot 10^{-5}$	6.2s	5.2s	2.8k	$4.1 \cdot 10^{-6}$	18
10^{-4}	$0.9 \cdot 10^{-4}$	$2.1 \cdot 10^{-6}$	40s	8.9s	43k	$2.6 \cdot 10^{-7}$	19
10^{-5}	$1.0 \cdot 10^{-5}$	$2.6 \cdot 10^{-7}$	429s	95s	332k	$2.7 \cdot 10^{-9}$	21

e_{des}	e_{meas}	$J_{final} - J_{acc}$	T_{total}	T_{hom}	n_Δ	μ_{final}	n_{hom}
10^{-2}	$0.5 \cdot 10^{-2}$	$4.2 \cdot 10^{-4}$	2.1s	1.6s	870	$3.7 \cdot 10^{-4}$	7
10^{-3}	$1.4 \cdot 10^{-3}$	$5.2 \cdot 10^{-5}$	6.8s	2.4s	7.0k	$2.3 \cdot 10^{-5}$	8
10^{-4}	$1.2 \cdot 10^{-4}$	$8.6 \cdot 10^{-6}$	48s	14s	42k	$7.8 \cdot 10^{-7}$	10
10^{-5}	$1.1 \cdot 10^{-5}$	$6.9 \cdot 10^{-7}$	732s	61s	522k	$5.4 \cdot 10^{-8}$	11

Figure 8: Computational results for the Neumann problem (top) and the Dirichlet problem (bottom).

6.2 Overall Performance

Let us now consider the overall performance of our algorithm for the two test problem. For a starting value $\mu_0 = 1$ and $(y_0, p_0) = (0, 0)$ we computed their solution for a variety of desired accuracies. As a coarse grid we used a uniform partitioning of the square, consisting of 8 triangles. Further, for both examples, we used the following algorithmic parameters. For the relative discretization accuracy (cf. (25)) we used $\Delta_{des} = 0.5$, as the relative accuracy for the corrector (cf. (31)) we used $\Lambda_{des} = 0.3$, and for the desired contraction (cf. (36)) we used $\Theta_{des} = 0.5$. The barrier function we used was a sum of a logarithmic barrier function and rational barrier functions up to order $q = 7$.

The numerical results showed in both examples that eventually the discretization error dominates the error introduced by the interior point regularization. Thus, after a sufficiently small homotopy error has been reached, it remaines to reduce the discretization error to a similar level, again with adaptive refinement. As it turned out, these final steps were (at least for medium and high accuracies) the steps which required (sometimes by far) most of the computational time. This is a very desirable property. It also indicates that the computational bottleneck is now the efficient solution of the large linear systems that arise towards the end of the algorithm. Here one should search for good iterative methods, which are robust with respect to the strong scaling by $b''(y; \mu)$ that appears towards the end of the algorithm.

Let us turn to the tables of results in Figure 8. Both problems were solved until the estimated total error was below desired accuracy e_{des}:

$$[\|y_{final} - y_{opt}\|_{L_2}^2 + \alpha^{-1} \|p_{final} - p_{opt}\|_{L_2}^2] \leq e_{des}^2.$$

Here (y_{final}, p_{final}) denotes the computed final solution. Comparison with a more accurate solution x_{acc} resulted in a measurement

$$e_{meas}^2 := \|y_{final} - y_{acc}\|_{L_2}^2 + \alpha^{-1} \|p_{final} - p_{acc}\|_{L_2}^2$$

and in a measurement $J_{final} - J_{acc}$ (with $J_{final} = J(y_{final}, \alpha^{-1} B^* p_{final})$) for the error in the objective functional.

Since it turned out that the discretization error was dominant for small μ, we used the following strategy. The homotopy was stopped, after the remaining length of the path was estimated to be well below the desired bounds. This goal was reached with n_{hom} homotopy steps at a homotopy parameter μ_{final} and required a computational time T_{hom}.

At this point of the algorithm, the nonlinearity of the problem was resolved well, but the discretization error was still larger than the accuracy requirement.

The remaining discretization error was reduced by some additional inexact Newton steps. In all examples, no more than two Newton steps were needed in this phase, and no more than 5 steps of adaptive refinement were performed. The overall algorithm required T_{total} computational time, and the final grid consisted of n_Δ triangles. Comparison of T_{hom} and T_{total} shows that for medium and high accuracies these last few steps consumed the dominant part of the computational time. This demonstrates the impact of adaptive grid refinement and careful accuracy matching on the efficiency algorithms for nonlinear problems in function space.

References

[1] M. Ainsworth and J.T. Oden. *A posteriori error estimation in finite element analysis*. Wiley, 2000.

[2] J.-J. Alibert and J.-P. Raymond. Boundary control of semilinear elliptic equations with discontinuous leading coefficients and unbounded controls. *Numer. Funct. Anal. and Optimization*, 3&4:235–250, 1997.

[3] E.L. Allgower, K. Böhmer, F.A. Potra, and W.C. Rheinboldt. A mesh-independence principle for operator equations and their discretizations. *SIAM J. Numer. Anal.*, 23:160–169, 1986.

[4] H. Amann. Nonhomogeneous linear and quasilinear elliptic and parabolic boundary value problems. In H.J. Schmeisser and H. Triebel, editors, *Function Spaces, Differential Operators and Nonlinear Analysis.*, pages 9–126. Teubner, Stuttgart, Leipzig, 1993.

[5] R. E. Bank and A. Weiser. Some a posteriori error estimators for elliptic partial differential equations. *Math. Comput.*, 44(170):283–301, 1985.

[6] P. Bastian, M. Blatt, C. Engwer, A. Dedner, R. Klöfkorn, S. Kuttanikkad, M. Ohlberger, and O. Sander. The Distributed and Unified Numerics Environment (DUNE). In *Proc. of the 19th Symposium on Simulation Technique in Hannover, September 12-14*, 2006.

[7] R. Becker, H. Kapp, and R. Rannacher. Adaptive finite element methods for optimal control of partial differential equations: Basic concept. *SIAM J. Control Optimization*, 39(1):113–132, 2000.

[8] R. Becker and R. Rannacher. An optimal control approach to a posteriori error estimation in finite element methods. *Acta Numerica*, 10:1–102, 2001.

[9] O. Benedix and B. Vexler. A posteriori error estimation and adaptivity for elliptic optimal control problems with state constraints. *Computational Optimization and Applications*, 2008.

[10] E. Casas. Control of an elliptic problem with pointwise state constraints. *SIAM J. Control Optimization*, 24:1309–1318, 1986.

[11] E. Casas. Boundary control of semilinear elliptic equations with pointwise state constraints. *SIAM J. Control Optim.*, 31:993–1006, 1993.

[12] E. Casas. Error estimates for the numerical approximation of semilinear elliptic control problems with finitely many state constraints. *ESAIM, Control Optim. Calc. Var.*, 8:345–374, 2002.

[13] E. Casas and M. Mateos. Uniform convergence of the FEM applications to state constrained control problems. *Comput. Appl. Math.*, 21(1):67–100, 2002.

[14] K. Deckelnick and M. Hinze. Convergence of a finite element approximation to a state-constrained elliptic control problem. *SIAM J. Numer. Anal.*, 45(5):1937–1953, 2007.

[15] K. Deckelnick and M. Hinze. A finite element approximation to elliptic control problems in the presence of control and state constraints. Technical Report Preprint HBAM2007-01, Hamburger Beiträge zur Angewandten Mathematik, Universtität Hamburg, 2007.

[16] K. Deckelnick and M. Hinze. Numerical analysis of a control and state constrained elliptic control problem with piecewise constant control approximations. In O. Steinbach K. Kunisch, G. Of, editor, *Numerical Mathematics and Advanced Applications, Proceedings of ENUMATH 2007, the 7th European Conference on Numerical Mathematics and Advanced Applications*, pages 597–604, Graz, Austria, September 2007, 2008. Springer.

[17] P. Deuflhard. *Newton Methods for Nonlinear Problems. Affine Invariance and Adaptive Algorithms*, volume 35 of *Series Computational Mathematics*. Springer, 2004.

[18] P. Deuflhard and M. Weiser. Local inexact Newton multilevel FEM for nonlinear elliptic problems. In M.-O. Bristeau, G. Etgen, W. Fitzgibbon, J.-L. Lions, J. Periaux, and M. Wheeler, editors, *Computational science for the 21st century*, pages 129–138. Wiley, 1997.

[19] I. Ekeland and R. Témam. *Convex Analysis and Variational Problems*. Number 28 in Classics in Applied Mathematics. SIAM, 1999.

[20] S. Goldberg. *Unbounded Linear Operators*. Dover Publications, Inc., 1966.

[21] A. Günther and M. Hinze. A posteriori error control of a state constrained elliptic control problem. *Journal of Numerical Mathematics*, 16(4):307–322, 2008.

[22] M. Hintermüller and R.H.W. Hoppe. Goal oriented mesh adaptivity for mixed control-state constrained elliptic optimal control problems. Technical Report Preprint Nr. 20/2008, Institut für Mathematik, Universität Augsburg, 2008.

[23] M. Hintermüller, K. Ito, and K. Kunisch. The primal-dual active set strategy as a semi-smooth Newton method. *SIAM J. Optim.*, 13:865–888, 2003.

[24] M. Hintermüller and K. Kunisch. Feasible and non-interior path-following in constrained minimization with low multiplier regularity. *SIAM J. Control Optim.*, 45(4):1198–1221, 2006.

[25] M. Hintermüller and M. Ulbrich. A mesh-independence result for semismooth Newton methods. *Math. Programming*, 101:151–184, 2004.

[26] M. Hinze and A. Schiela. Discretization of interior point methods for state constrained elliptic optimal control problems: Optimal error estimates and parameter adjustment. Technical Report SPP1253-08-03, Priority Program 1253, German Research Foundation, 2007.

[27] A. Hohmann. *Inexact Gauss Newton Methods for Parameter Dependent Nonlinear Problems*. PhD thesis, Free University of Berlin, Dept. Math. and Comp. Sci., 1994.

[28] R.H.W. Hoppe and M. Kieweg. A posteriori error estimation of finite element approximations of pointwise state constrained distributed control problems. *SIAM J. Control Optim.*, submitted, 2007.

[29] B. Kummer. Generalized Newton and NCP-methods: convergence, regularity and actions. *Discussiones Mathematicae - Differential Inclusions*, 20(2):209–244, 2000.

[30] C. Meyer. Error estimates for the finite element approximation of an elliptic control problem with pointwise constraints on the state and the control. *Control and Cybernetics*, 37:51–85, 2008.

[31] C. Meyer, F. Tröltzsch, and A. Rösch. Optimal control problems of PDEs with regularized pointwise state constraints. *Computational Optimization and Applications*, 33:206–228, 2006.

[32] U. Prüfert, F. Tröltzsch, and M. Weiser. The convergence of an interior point method for an elliptic control problem with mixed control-state constraints. ZIB Report 04-47, Zuse Institute Berlin, 2004. to appear at Computational Optimization and Applications.

[33] E. Schechter. *Handbook of Analysis and its Foundations*. Academic Press, 1997.

[34] O. Schenk and K. Gärtner. Solving unsymmetric sparse systems of linear equations with PARDISO. *J. of Future Generation Computer Systems*, 20(3):475–487, 2004.

[35] A. Schiela. *The Control Reduced Interior Point Method - A Function Space Oriented Algorithmic Approach.* PhD thesis, Free University of Berlin, Dept. Math. and Comp. Sci., 2006.

[36] A. Schiela. Convergence of the control reduced interior point method for PDE constrained optimal control with state constraints. ZIB Report 06-16, Zuse Institute Berlin, 2006.

[37] A. Schiela. Barrier methods for optimal control problems with state constraints. ZIB Report 07-07, Zuse Institute Berlin, 2007.

[38] A. Schiela. An extended mathematical framework for barrier methods in function space. ZIB Report 08-07, Zuse Institute Berlin, 2008.

[39] A. Schiela. An interior point method in function space for the efficient solution of state constrained optimal control problems. ZIB Report 07-44, Zuse Institute Berlin, 2008.

[40] M. Ulbrich. Semismooth Newton methods for operator equations in function spaces. *SIAM J. Optim.*, 13:805–842, 2003.

[41] S. Volkwein and M. Weiser. Affine invariant convergence analysis for inexact augmented Lagrangian-SQP methods. *SIAM J. Control Optim.*, 41(3):875–899, 2002.

[42] M. Weiser. *Function Space Complementarity Methods for Optimal Control Problems*. PhD thesis, Free University of Berlin, Dept. Math. and Comp. Sci., 2001.

[43] M. Weiser, A. Schiela, and P. Deuflhard. Asymptotic mesh independence of Newton's method revisited. *SIAM J. Numer. Anal.*, 42(5):1830–1845, 2005.

[44] D. Werner. *Funktionalanalysis*. Springer, 3rd edition, 2000.

[45] W. Wollner. A posteriori error estimates for a finite element discretization of interior point methods for an elliptic optimization problem with state constraints. *Computational Optimization and Applications*, 2008.

[46] E. Zeidler. *Nonlinear Functional Analysis and its Applications*, volume II/A. Springer, New York, 1990.